UNIVERSITÀ DEGLI STUDI DI PARMA

Dottorato di ricerca in Scienze Chimiche

Ciclo XXVI (2011-2013)

Study of the behavior of organic and organometallic crystalline materials

Supervisor:

Prof. ssa Alessia Bacchi

Co-Supervisor:

Prof. Alberto Girlando

Dottorando:

Domenico Crocco

To my mother
and my cousin

INTRODUCTION

1. Supramolecular chemistry

It is very difficult to give a definition of supramolecular chemistry[1]. In his Nobel lecture[2], Jean-Marie Lehn defined the field as follows:

"[…] Supramolecular chemistry is the chemistry of the intermolecular bond, covering the structures and functions of the entities formed by association of two or more chemical species.[…]"

This means that the supramolecules are combinations of molecules that come together, either spontaneously or by design, to form a larger unit with properties resulting from the original components. Braga[3] has given the following definition: "Supramolecular chemistry has dissolved all the traditional barriers between the subdivisions of chemistry…focusing attention on the *collective* properties". Supramolecular chemistry is very interesting because embraces all areas of chemistry in order to study the properties of different compounds for possible practical application.
When these methods are specifically applied to crystalline solids, it leads to the area of crystal engineering[4].

[1] J. W. Steed, in *Encyclopedia of supramolecular chemistry*, eds. J. L. Atwood and J. W. Steed, Marcel Dekker, Inc., New York, 2004, vol. 2, pp. 1401 - 1419
[2] J.-M. Lehn, *Angew. Chem., Int. Ed. Engl.*, 1988, **27**, 89 - 112
[3] D. Braga, *Chem. Commun.*, 2003, 2751 - 2754
[4] G. R. Desiraju, *Angew. Chem. Int. Ed.*, 2007, **46**, 8342-8356.| (b) D. Braga and F. Grepioni Eds., *Making Crystal by Design: Methods, Techniques and Applications*. WILEYVCH, Weinheim, 2007

2. Crystal engineering

Crystal engineering is the rational design of molecular solids[4], it can be regarded as a solid-state supramolecular chemistry and it goes far beyond the traditional divisions of organic and inorganic chemistry, thus resulting in an extraordinary blend of ideas and techniques.

"[…] Molecular crystals have interesting physical and chemical properties that are not associated with other categories of crystalline substances. These properties are connected to, and closely related to, their internal periodic structures. These internal structures are known as crystal structures and they are of outstanding importance in crystal engineering. So, there is a need to be able to design particular crystal structures, wherein molecules are assembled in particular ways. A particular crystal structure, in turn, has a particular property that is desired. Crystal engineering therefore consists of many different operations. These include the determination of crystal structures, the understanding or analysis of these and other know crystal structures, the use of this understanding trying to design a crystal structure of a particular type of including hitherto unknown structure types, the actual crystallization experiment, and finally the realization of a pre-desired crystal property. Clearly, many skills are involved in the art and science of crystal engineering. We will now trace the historical background of the several scientific stream of thought that have come together in this new subject. […]"[4].

3. Polymorphism

McCrone[5] defined polymorphism as the capability of the same chemical compound to crystallize "[…] as more than one distinct crystal species […]". This means that the same compound can pack in different ways in the solid state. This phenomenon is important for several industries such as pharmaceutical, food, pigments and materials. The properties of a certain compound generally depend by its packing, therefore a change in the structure can give the same chemical compound new properties. This has major implications for patents on drugs where a new polymorph might, for example, have better solubility properties[7,8]. The polymorph is considered to be a new compound; therefore a rival company can attain a patent for it subsequently costing other companies millions[6,7].

Desiraju[8] posed an excellent question regarding the abundance of polymorphism:

"[…] Why should any molecule crystallize in more than one form especially when it appears that molecular recognition is such a subtle and specific event that demands an exact matching in geometrical and chemical terms of the various interacting molecules? […]"

Therefore, the study of this phenomenon is of utmost importance. The study of these systems allow crystal engineers to understand what controls molecular assembly and, in turn, uses these principles to engineer specific compounds with specific properties. Crystallization is a process that is

[5] W. C. McCrone, in *Physics and chemistry of the organic solid state*, eds. D. Fox, M. M. Labes and A. Weissberger, Interscience, 1965, vol. 2, pp. 726 - 766
[6] J. Bernstein, *Polymorphism in Molecular Crystals*, Oxford University Press, New York, 2008
[7] A. Nangia, *Acc. Chem. Res.*, 2008, **41**, 595 - 604
[8] G. Desiraju, *J. Chem. Sci.*, 2010, **122**, 667 - 675

dependent on the formation of nucleation sites within the crystallization vessel. This process is dependent on the temperature, solvent system and the rate at which crystallization is allowed to occur[9]. Changing these experimental conditions can lead to the formation of polymorphs.

Molecular structure is determined by bond lengths, bond angles and torsion angles[9]. These torsion angles allow some molecules a large degree of freedom of movement[10], which allows them to adopt different conformations in the solid state[10]. This is termed *conformational polymorphism*. However, the more important contribution is that they provide the opportunity to study the relationship between intra- and intermolecular energies[9]. In some cases two or more polymorphs may appear under the same conditions, often crystallizing in the same vessel[9]. This is defined as *concomitant polymorphism*. This is due to the fact that concomitant polymorphs are almost energetically equivalent. Since there appear to be conditions that both polymorphic forms favour, to study concomitant polymorphs leads to a wealth of information regarding the control of polymorphic crystallization.

The relationship between two polymorphs can be classified into two systems: enantiotropic or monotropic. This classification is related to the Gibbs free energy (G) of the system.

[9] M. R. Caira, in *Encyclopedia of supramolecular chemistry*, eds. J. L. Atwood and J. W. Steed, M. Dekker, 2004, vol. 2, p. 1129

[10] M. Lefenfeld, *et. al.*, Adv. Mater. 15, 1188 (2003)

4. Polymorphism of molecular materials

Recently, π-conjugated oligomers as oligoacenes, oligophenylenes and oligothiophenes have been extensively studied to obtain a new generation of organic-based devices. Their properties are suitable for use in transistors, light emitting diodes, laser and nonlinear optical devices[11,11,12] Organic semiconductors have many advantages over their inorganic counterparts. They offer the possibility to be solution-processed allowing the fabrication of devices such as circuits, displays on plastic substrate. They can also deposited by unconventional methods, such as inkjet and screen printing. Organic[13] semiconductors such as pentacene and rubrene have surpassed amorphous Si in performance, and their use as the semiconducting layer in field-effect transistors (FETs) represent another pole of high technological relevance[14]. Although thin film or polymers form are the most suitable for the practical use of such materials, the optimization of the device performances stimulates the research towards understanding intrinsic properties, a goal that can be achieved through the study of single crystals.

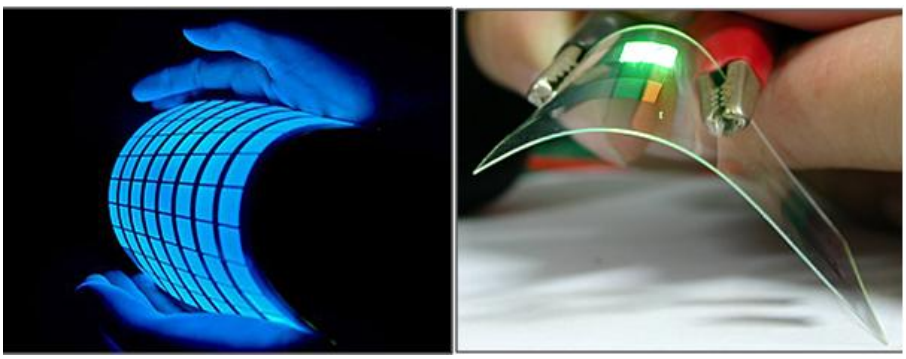

Figure 1 Typical pictures of OLEDs

[11] M. Lefenfeld, *et. al.*, Adv. Mater. 15, 1188 (2003)

[12] H. E. A. Huitema, *et. al.*, Nature 414, 599 (2001)

[13] A. Brillante, I. Bilotti, R. G. Della Valle, E. Venuti, A. Girlando, CrystEngComm 10, 937 (2008)

[14] G. R. Desiraju, *CrystEngComm*, 2003, **5**, 466 - 467

However, organic materials present different problems: the chemical purity of the sample, improved by purification techniques, and the polymorphism in the crystalline arrangement. Spectroscopic investigations in the region of lattice phonons have been shown to be a powerful technique in the identification of phase purity[14]. It is a easy, non destructive and fast experimental tool for in-situ characterization. Furthermore the investigation of the vibrational structure of organic semiconductors gives us some insight about the role of phonons in the absorption and luminescence optical processes and in their electric transport properties.

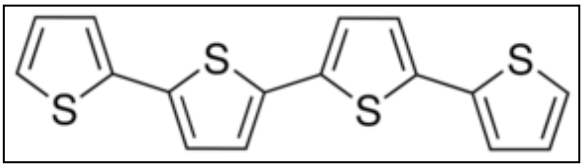

Figure 2 α-quaterthiophene

5. Co-crystals

There has been much debate about how to define this term[15]. Dunitz described the co- in co-crystal as indicating "togetherness"[15] i.e. a crystal structure formed by two or more components.

For the purpose of this study, the term "co-crystal" will be defined as a multicomponent molecular crystal as described by Bond[16].

It is unfortunately not a simple exercise to prepare co-crystals. The point is that the interactions between the heteromeric molecules must be favored than the interactions between homomeric molecules. In order to form co-crystals is necessary to understand the interactions between functional

[15] J. D. Dunitz, *CrystEngComm*, 2003, **5**, 506 - 506
[16] A. Bond, *CrystEngComm*, 2007, **9**, 833 - 834

groups. This understanding will guide the choice of co-crystal formers used in co-crystallization experiments.

6. Supramolecular synthons

In crystal engineering it is very important to identify the intermolecular interactions that guide the solid-state structure of crystals[17]. Desiraju was the first to define the term supramolecular synthon as "structural units within supermolecules which can be formed and/or assembled by known or conceivable synthetic operations involving intermolecular interactions"[17,18]. A synthon is therefore derived from designed combinations of interactions[18]. This is illustrated in Fig. 3. The carboxylic acid moiety hydrogen bonds to the complementary carboxylic acid moiety of another molecule to form the well-known carboxylic acid dimer[19]. This spatial arrangement of an intermolecular interaction is termed a supramolecular synthon[20]. These supramolecular synthons are dependent on the types of intermolecular interactions that occur in the solid state. Fig. 4 illustrates a selection of other supramolecular synthons.

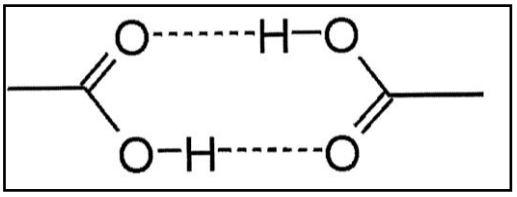

Figure 3

[17] G. R. Desiraju, *Angew. Chem., Int. Ed. Engl.*, 1995, **34**, 2311 - 2327
[18] V. R. Thalladi, B. S. Goud, V. J. Hoy, F. H. Allen, J. A. K. Howard and G. R. Desiraju, *Chem. Commun.*, 1996, 401 - 402
[19] G. Desiraju, *J. Mol. Struct.*, 2003, **656**, 5 - 15
[20] A. Nangia and G. Desiraju, in *Design of Organic Solids*, eds. E. Weber, Y. Aoyama, M. Caira, G. Desiraju, J. Glusker, A. Hamilton, R. Meléndez and A. Nangia, Springer Berlin / Heidelberg, 1998, vol. 198, pp. 57 - 95

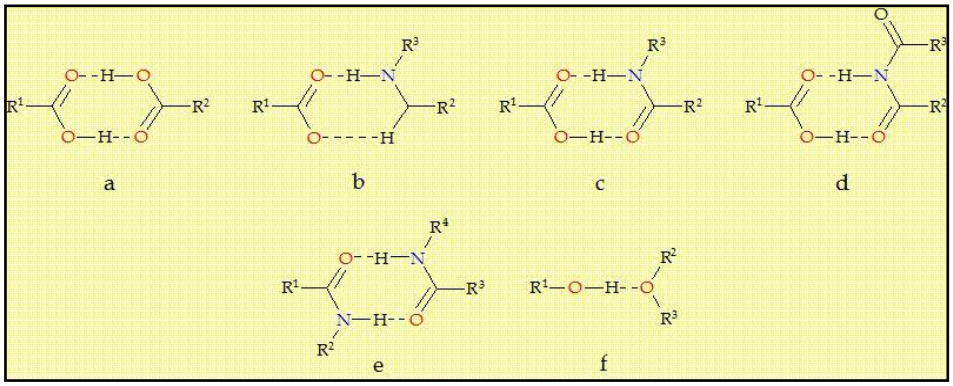

Figure 4

7. Intermolecular interactions

The intermolecular interactions hold the crystal structure together. These interactions are specifically defined as being between atoms that are not directly bonded[21]. Intermolecular interactions are classified according to their strength with respect to distance and their directionality[21]. Long-range forces include heteroatom interactions, namely interactions among N, O, S, Cl, Br, I or any of these atoms and carbon or hydrogen[21,22]. Medium-range forces generally govern close-packing, and include interactions such as C-H, C-C and H-H interactions[22]. These interactions generally lead to a minimization of the free energy of the crystal lattice[23]

7.1. Van der Waals forces and close packing

Van der Waals interactions occur as a consequence of London dispersion, ie the polarization of molecular electron clouds results in weak electrostatic intermolecular attractive phenomena. The value for this type of interaction is variable, but generally less than 5 kJ/mol. These types of interactions include the induced dipole to induced dipole, or London forces. Van der Waals is an interesting interaction for assembly of molecules in the solid state, but they are unfortunately not strongly directing interactions. The interactions between attractive and repulsive forces allows molecules to orientate themselves in such a way as to utilize all available space and pack efficiently.

[21] G. Desiraju, in *Solid-state supramolecular chemistry: crystal engineering*, eds. D. D. MacNicol, F. Toda and R. Bishop, Pergamon, Oxford, 1996, vol. 6, p. 1
[22] G. R. Desiraju, *Angew. Chem., Int. Ed. Engl.*, 1995, **34**, 2311 - 2327
[23] J. Glusker, in *Design of organic solids*, ed. E. Weber, Springer-Verlag Berlin Heidelberg, Germany, 1998, vol. 198, pp. 3 - 56

7.2. The hydrogen bond

The hydrogen bond is the most well-known intermolecular interaction in crystal engineering[24]. It can be written as X-H···A with X being the donor and A the acceptor[25]. It is such a well-known interaction due to the fact that it is relatively strong and suitably directional[26]. If a molecule contains a functional group that has the ability to form a hydrogen bond, it will always do so, unless there are factors such as steric hindrance that prohibit this from happening[26].

These bonds can be classified as very strong, strong and weak. This depends if the hydrogen bond in question can direct the aggregation of the molecules in any crystal structures obtained[26]. The strength of the hydrogen bond is also dependent on the atoms that are involved in the hydrogen bond[26]. For neutral molecules the typical values for a hydrogen bond are in the range of 10 – 65 kJ mol^{-1}, however, the strength of the interaction can increase to 80 – 120 kJ mol^{-1} [27]. Weak hydrogen bonds involve interactions between O-H···Ph and C-C-H···O[26], these weaker bonds can however still play an important role in directing the aggregation of molecules in the solid state[27, 26].

7.3. π-π Stacking interactions

This type of interaction occurs between aromatic rings and ranges in the value of 0 – 50 kJ mol^{-1} [28] These interactions can be divided into two types: face-to-face and edge-to-face[28]. It has been shown that this stacking

[24] G. Desiraju, J. J. Vittal and A. Ramanan, *Crystal engineering: a textbook*, World Scientific Publishing Co. Pte. Ltd., Singapore, 2011
[25] G. R. Desiraju, in *Encyclopedia of supramolecular chemistry*, eds. J. L. Atwood and J. W. Steed, Marcel Dekker, Inc., New York, 2004, vol. 1, pp. 658 - 672
[26] C. B. Aakeröy and D. S. Leinen, in *Crystal engineering: from molecules and crystals to materials*, eds. D. Braga, F. Grepioni and A. G. Orpen, Kluwer Academic Publishers, Netherlands, 1999, vol. 538, pp. 89 - 106
[27] M. C. Etter, *J. Phys. Chem.*, 1991, **95**, 4601 - 4610
[28] J. W. Steed and J. L. Atwood, *Supramolecular chemistry*, John Wiley & Sons, Ltd., West Sussex, 2000

interaction is due to the interaction between a positive σ-framework of one molecule and the negatively charged π-cloud of the other molecule[29].

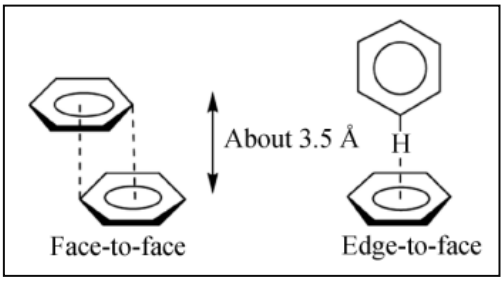

Figure 5 The two types of π-π stacking interactions

7.4. Halogen bonding

This term describes the donor-acceptor interactions of halogen atoms that play the role of Lewis acid[30]. The halogens can form interactions with other halogen atoms, or with carbon or nitrogen atoms. The angle of the intermolecular halogen bond generally is in the range from 160° to 180°, even for weak interactions where the interaction distance is greater than 3 Å[31].

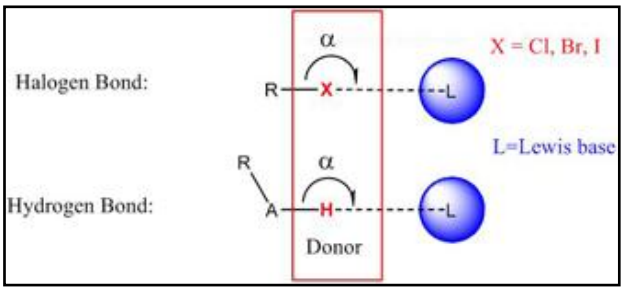

Figure 6 Halogen bonding

[29] C. A. Hunter and J. K. M. Sanders, *J. Am. Chem. Soc.*, 1990, **112**, 5525 - 5534
[30] P. Metrangolo and G. Resnati, in *Encyclopedia of supramolecular chemistry*, eds. J. L. Atwood and J. W. Steed, Marcel Dekker, Inc., New York, 2004, vol. 1, pp. 626 – 635

8. Crystallization and Crystal Growth

Crystallization of molecules in solution is also a supramolecular process. It is a complex but highly efficient process in which a number of molecular groups compete with each other to be sites for intermolecular interactions that might lead to a stable crystal structure. A kinetic process is usually described using the reagent concentration as the driving force for the chemical rate process; however, in the case of crystallization, the concentration range over which the process can occur is limited by the equilibrium composition of the system corresponding to the conditions chosen[32].

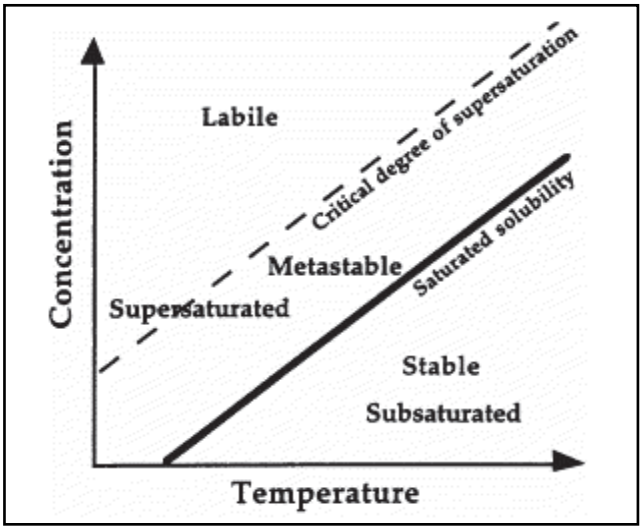

Figure 7 Solubility diagram for a solid

In Figure 7 is reported a hypothetical solubility curve: if the composition of the solution lies below the solubility curve, the existing crystals will dissolve because the solution is undersaturated. On the other hand, a solution lying above the curve is defined supersaturated, since the amount of dissolved solute is greater than the equilibrium saturation value, only in

this region crystals can form and grow: we can conclude that supersaturation is the driving force for the crystallization process. For better understanding it is convenient to consider crystallization occurring in two steps, nucleation and growth. According to the Classical Nucleation Theory, nucleation is the process of generating crystal nuclei inside a large volume of the metastable solution phase; this transformation requires crossing a free energy barrier. If we consider the variation of ΔG during the formation of a nucleus, defined as the difference between the free energy of the molecule of the bulk (ΔG_V) and that of the surface (ΔG_S), we can observe in Figure 8 that at very small sizes it is a positive term, and many of the aggregating molecules will tend to reside at the surface making the nucleus unstable, causing its dissolution. Once the nucleus gets sufficiently large, the decrease in free energy associated with formation of the bulk phase becomes high enough that the hindrance offered by the interfacial energy is not important: at this stage, addition of a molecule to the nucleus lowers the free energy. This intermediate size, known as the critical size, represents the activation barrier of this stage and it is strongly dependent from supersaturation.

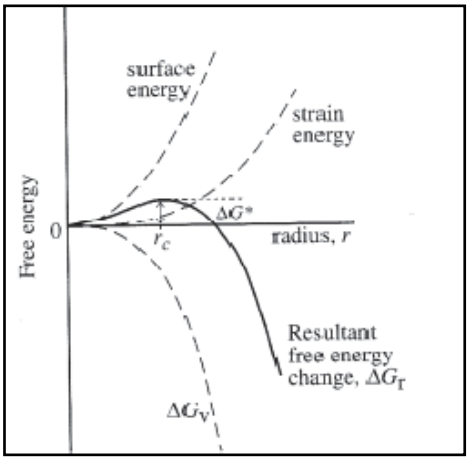

Figure 8 Variation of ΔG with the size of the nucleus

The following growth step can be described as the diffusion of the growth units (solute molecules) from the surrounding supersaturated solution to the surface of the critical nucleus and their incorporation into the structure of the crystal lattice; the rate-controlling step for growth is therefore the rate of diffusion of these building blocks. Crystallization from a solution, which can be considered the most common case, can be achieved by reducing the solubility of the solute in order to reach the supersaturation zone: this can be done by cooling the solution, by slowly evaporating the solvent or by adding a suitable antisolvent.

9. Gas Storage in Porous Materials

Gas storage is a very important topic at the moment with applications for environmental issues and in energy storage. Gases can be stored in materials such as activated carbon[31,32] and metal oxides[33,34]. However, the most utilized are zeolites and metal organic frameworks. The main advantages that these types of materials have over others is their large surface areas, with zeolites achieving several hundred m^2g^{-1} and some MOFs exceeding $5000m^2g^{-1}$.[35,36].

The metal sites in both zeolites and MOFs also provide an area for the gas to bind to if it can be "activated". During this process the material is heated to remove guests present from the synthesis process. Care must be taken during this process as incomplete removal of the guest molecules can result in lower than expected storage capacities[37]. Sometimes, the removal of guest molecules can result in the breakdown of the framework.

[31] F. Rodríguez-Reinoso, Y. Nakagawa, J. Silverstre-Albero, J.M. Juárez-Galán and M. Molina- Sabio, Microporous and Mesoporous Materials, 2008, 115, 603-608
[32] M. J. Prauchner and F. Rodríguez-Reinoso, Microporous and Mesoporous Materials, 2008, 109, 581-584
[33] J. Ma, Z. Liu, Q. Liu, S. Guo, Z. Huang and Y. Xiao, Fuel Processing Technology, 2008, 89, 242-248
[34] J. Pasel, P. Käßner, B. Montanari, M. Gazzano, A. Vaccari, W. Makowski, T. Lijewski, R. Dziembaj and H. Papp, Applied Catalysis B: Environmental., 1998, 18, 199-213
[35] G. Féréy, C. Mellot-Draznieks, C. Serre, F.Millange, J. Dutour, S.Surble, and I. Margiolaki, Science., 2005, 309, 2040-2042
[36] H.K. Chae, D.Y. Siberio-Prez, J. Kim, Y. Go, M. Eddaoudi, A.J. Matzger, M. O'Keeffe, and O.M. Yaghi, Nature, 2004, 427, 523-527
[37] B. Xiao, P. S. Wheatley, X. Zhao, A. J. Fleycher, S. Fox, A. G. Rossi, I.L. Megason, S. Bordiga, L. Regli, K. M. Thomas, and R.E. Morris, J. Am. Chem. Soc., 2007, 129, 1203-1209 Science, 2007, 315, 18281-1831

PART I: The polymorphism of TPB

1. The first four polymorphs of TPB

The study of polymorphism and solid forms is of great importance in crystal engineering in various areas such as the pharmaceutical and materials science. Polymorphs are characterized by the same chemical composition but by mutually different molecular conformations and crystal packing, for this reason they may exhibit different properties in the solid state.

In my thesis work I have mainly worked on the polymorphism of 1,1,4,4-tetraphenyl-1,3-butadiene (TPB).

TPB is a material that emits efficiently in the blue, whose photoluminescence properties have been investigated in solution and in the polymer matrix.

The emission remains good even in the crystalline state, but studies about solid state properties of this material do not exist[38].

1.1 Crystal packing and morphology

TPB crystallizes in different polymorphs which have different conformation and different packing.

[38] Girlando, A.; Iannelli, S.; Bilotti, I.; Brillante, A.; Della Valle, R,G.; Venuti, E.; Campione, M.; Mora, S.; Silvestri, L.; Spearman, P.; Silvia, T. *Cryst. Growth Des.*, **2010**, *10* (6), pp 2752–2758

α-TPB

The α polymorph has been obtained by crystallization from saturated solutions in different solvents hexane, cyclohexanone, pentane, chloroform, ethanol, methanol. The morphology of α-TPB obtained by different methods is shown in Fig. 9.

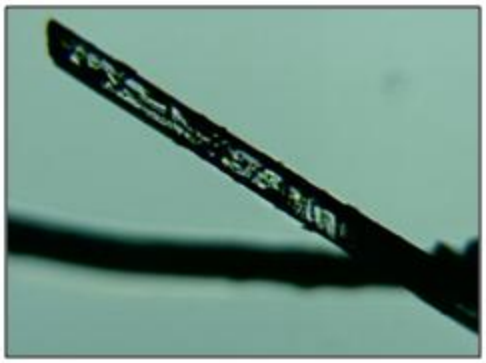

Figure 9 The alpha phase morphology

The α-TPB crystallizes in the monoclinic $P2_1$ space group, with two molecules in the unit cell.

In Fig. 10, 11, 12 I report the packing of the α form along the crystallographic axes a, b and c respectively.

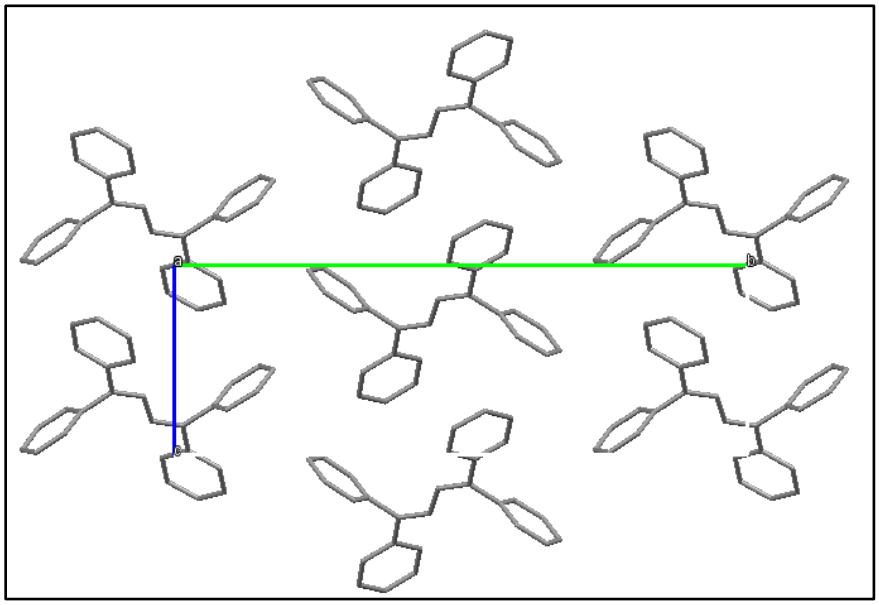

Figure 10 View along a

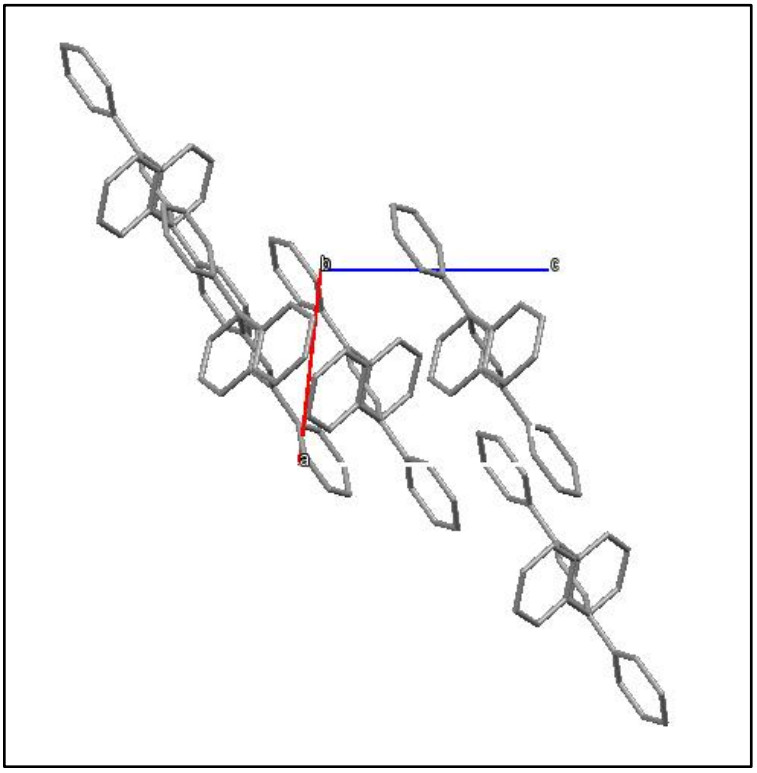

Figure 11 View along b

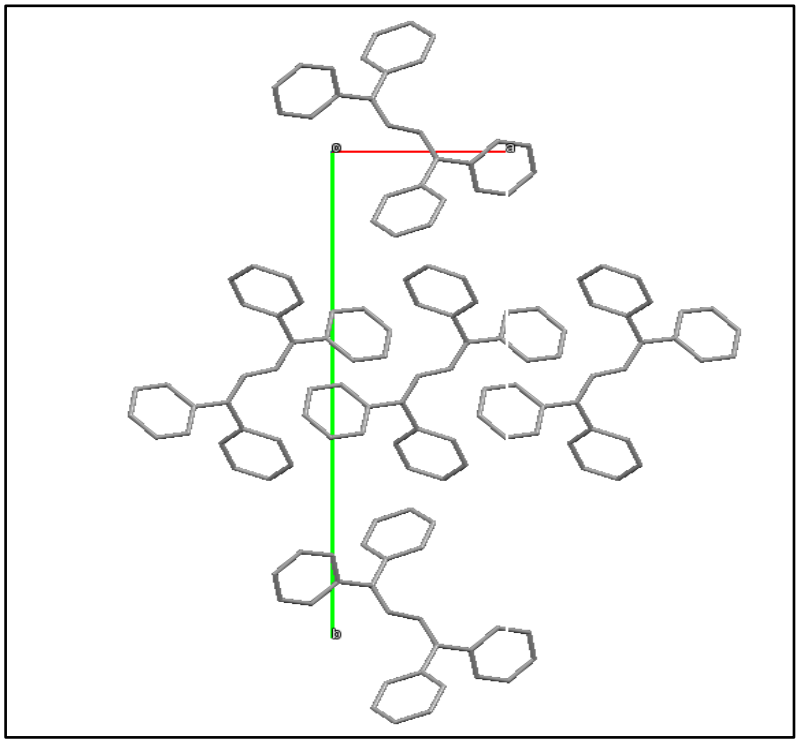

Figure 12 View along c

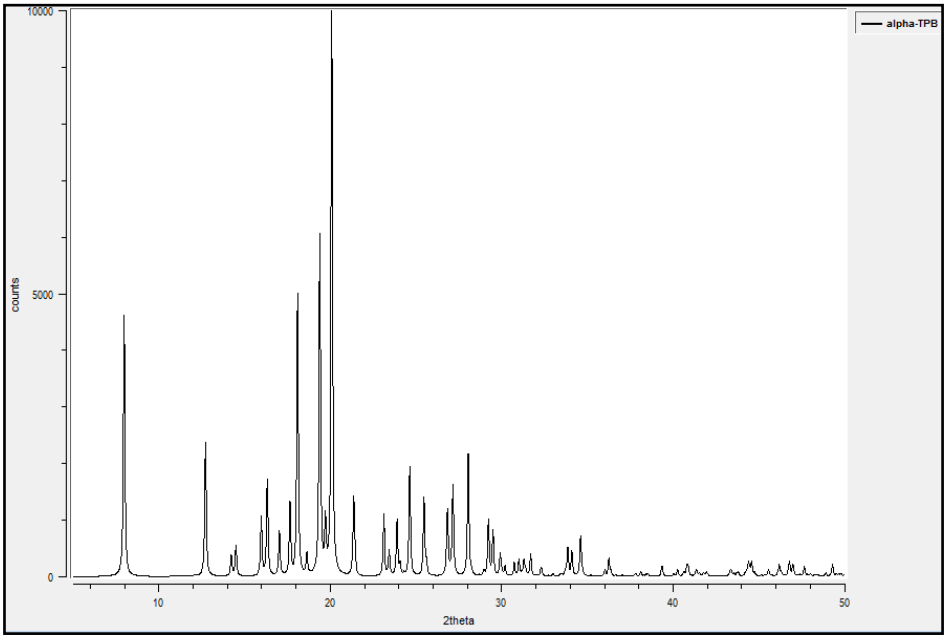

Figure 13 The alpha phase powder pattern

β- TPB

β-TPB has only be obtained by physical vapor transport method[39], but it has always been obtained together with the α phase. Obtaining large single crystals from those procedure is therefore difficult. The morphology of β-TPB is shown in Fig. 14.

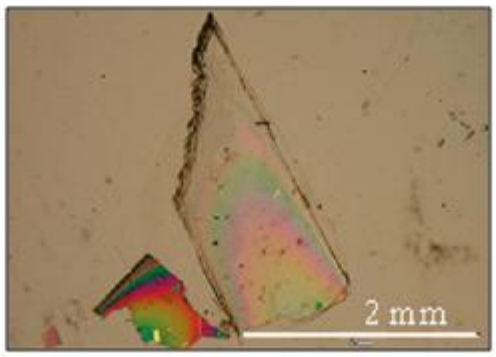

Figure 14 The beta phase morphology

The solid state packing of beta form crystallized in a monoclinic $P2_1/c$ space group.

In Fig. 15, 16, 17 I report the packing of the β phase along the crystallographic axes a, b and c respectively.

[39] A. Bacchi, G. Cantoni, F. Mezzadri, P. Pelagatti, Cryst. Growth Des., 2012, 12, 4240–4247

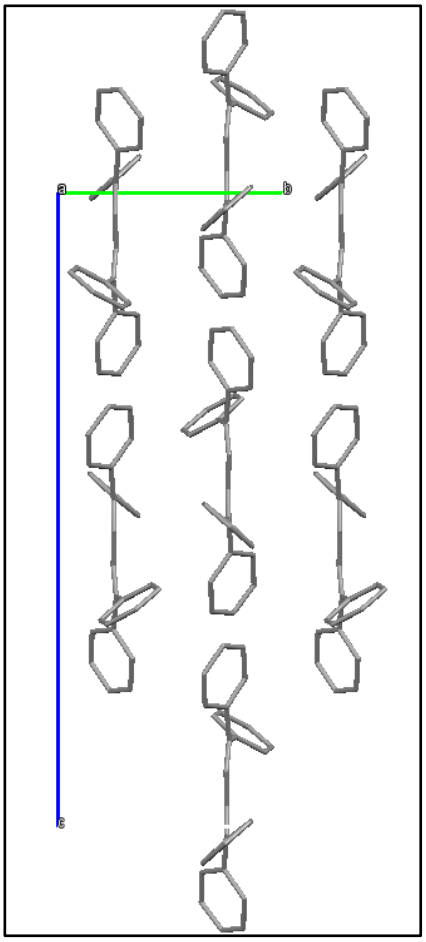

Figure 15 View along a

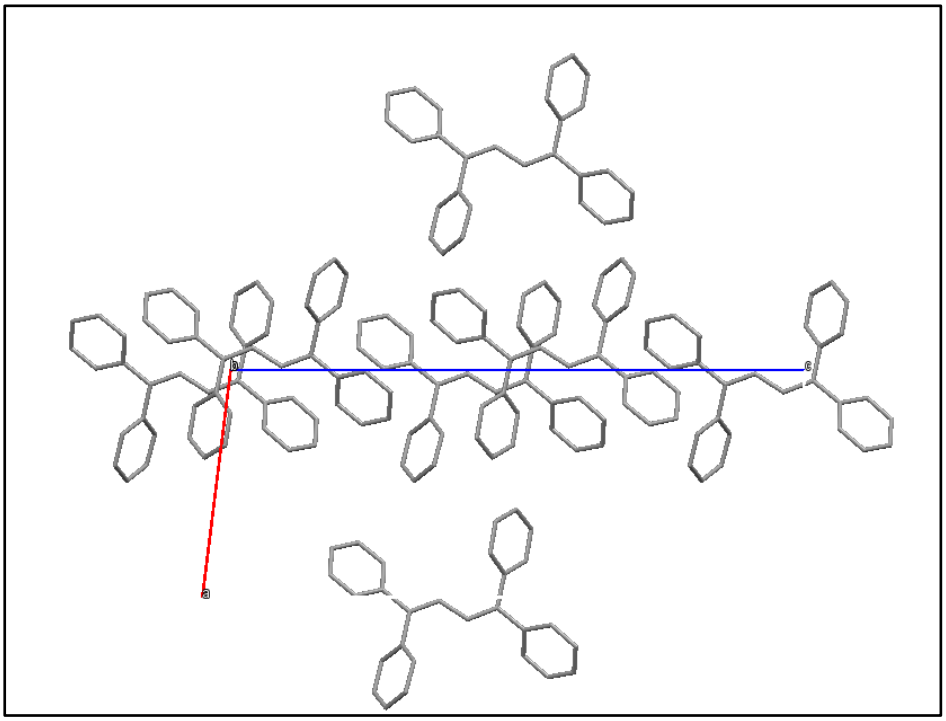

Figure 16 View along b

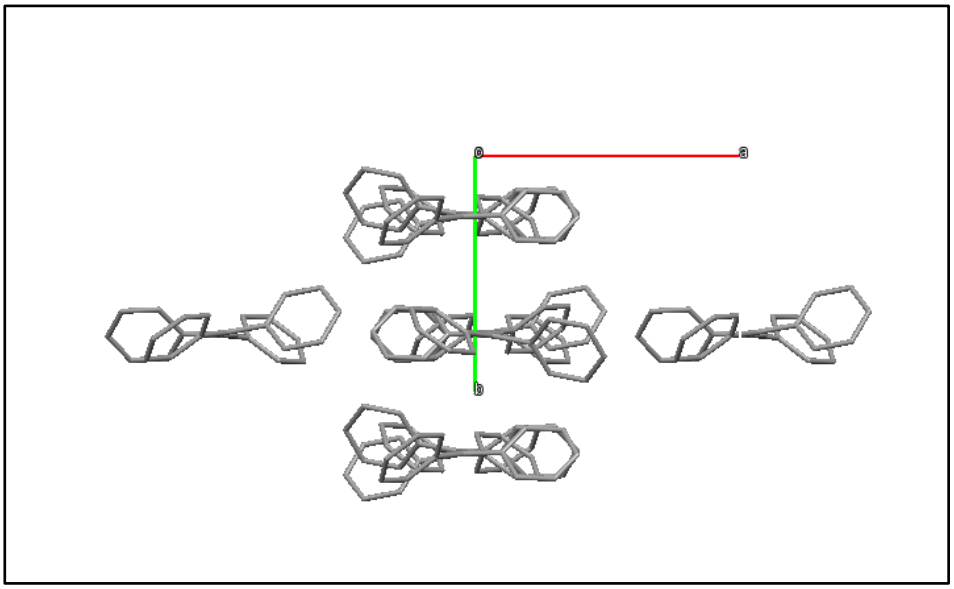

Figure 17 View along c

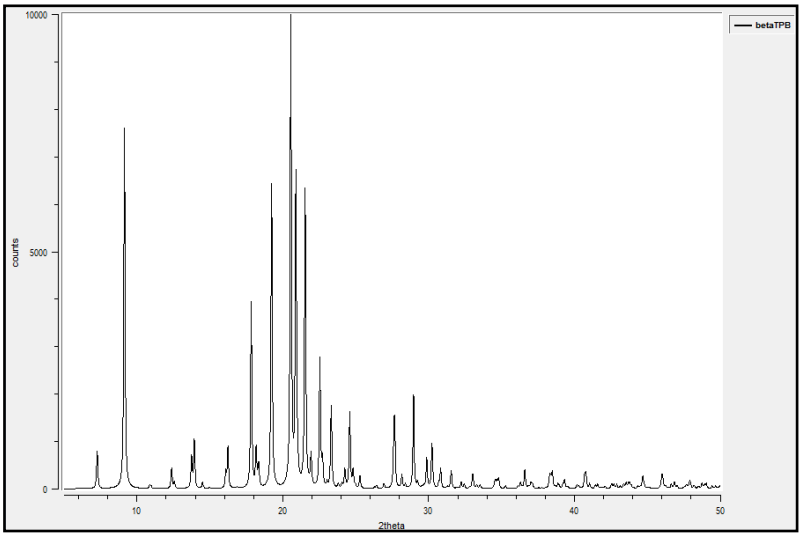

Figure 18 The beta polymorph powder pattern

The β-phase shows ASE (amplified stimulate emission), which constitutes the necessary prerequisite to build a laser: this derives from the fact that the transition dipole moments of lowest energy electronic transition is directed along the butadiene chains, and these are all aligned.

γ- TPB

γ-TPB has been obtained only twice by crystallization from ethyl- or butyl-acetate. However, this method is not reproducible.

The typical prismatic morphology is shown in Fig. 19.

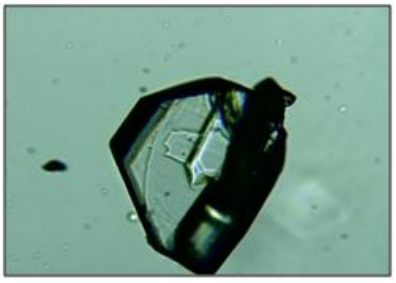

Figure 19 Gamma phase morphology

γ-TPB crystallizes in the triclinic P-1 space group, with two molecules per unit cell.

In Fig. 20, 21, 22 I report the packing of the γ form along the crystallographic axes a, b and c respectively.

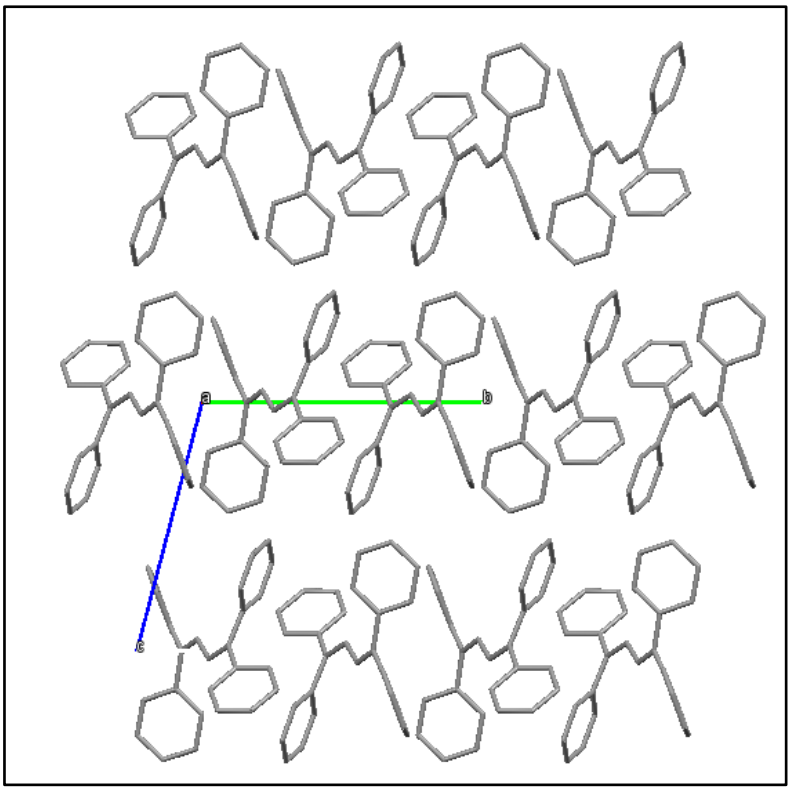

Figure 20 View along a

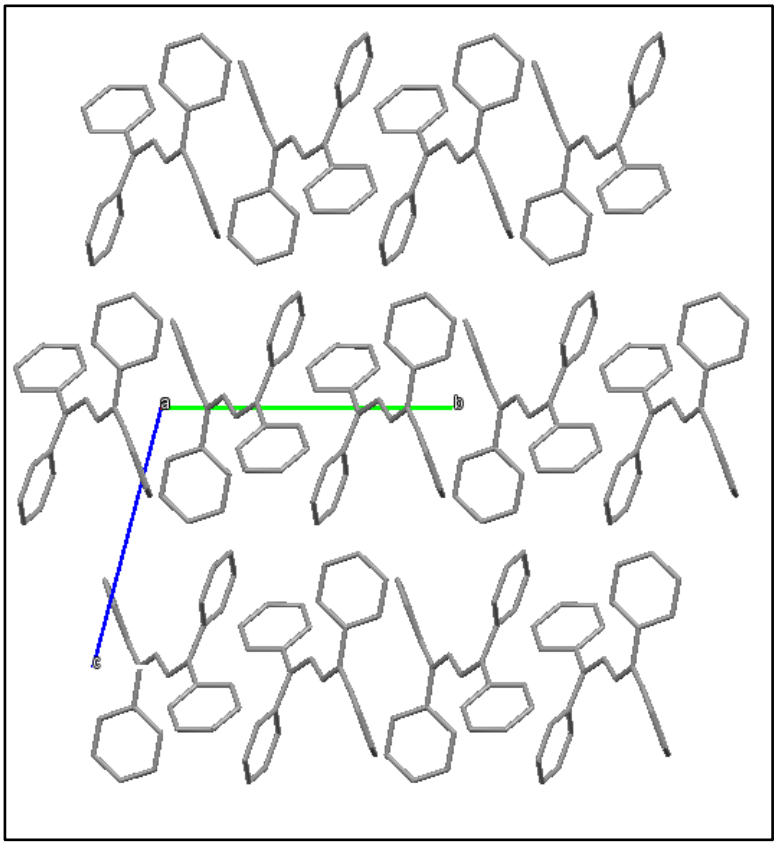

Figure 21 View along b

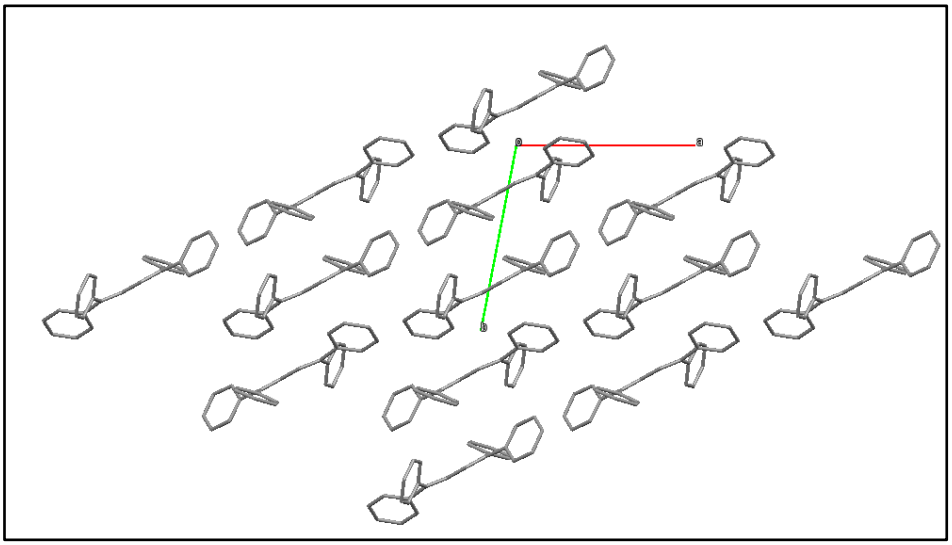

Figure 22 View along c

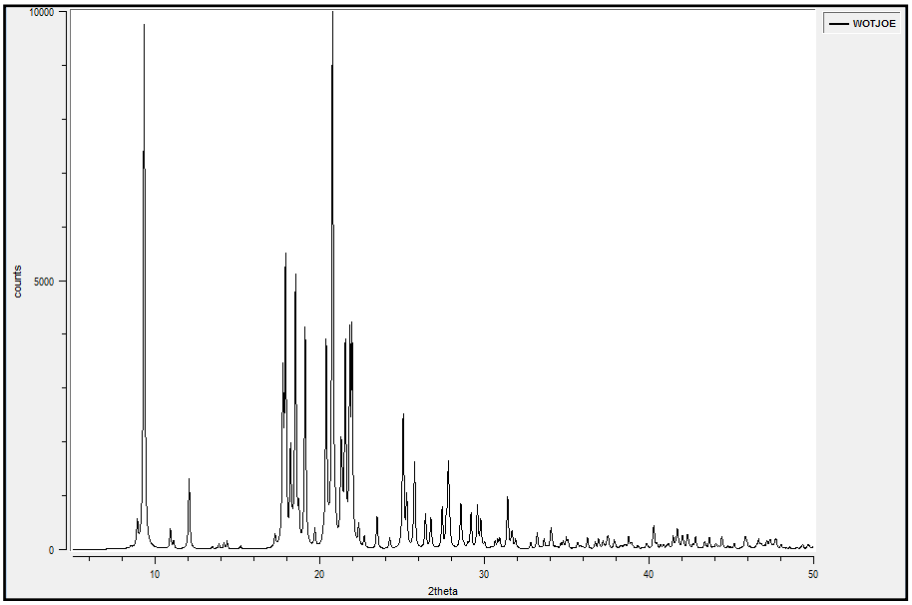

Figure 23 The gamma phase powder pattern

We have discovered a new method to obtain γ-TPB via the technique of the cold finger (Fig.24). Crystals of TPB were sublimated in presence of crystals of γ phase (Fig. 25), successively microcrystals of gamma phase were formed on the surface of the seed. This result has been demonstrated by Raman spectroscopy (see Appendix).

Figure 24 The cold finger

The α polymorph is instead crystallized on the walls of the cold finger in form of microcrystals. Subsequent experiments have led always the same results, confirming the reproducibility of the method. The sublimation of TPB in absence of crystals of γ polymorph leads to the crystallization of α-TPB.

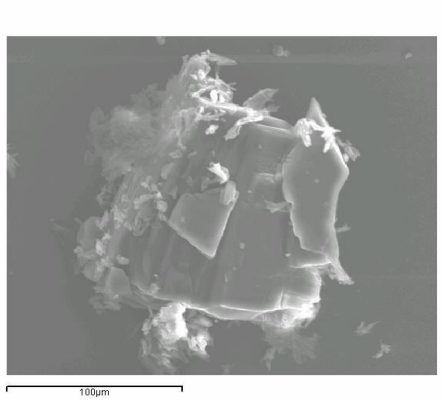

Figure 25 Image of γ-TPB after sublimation process by cold finger

For us it was very important to find the conditions for the growth of the γ-phase because it presents similar packing and the same parallel disposition of transition dipole moments of β-phase (Fig 26).

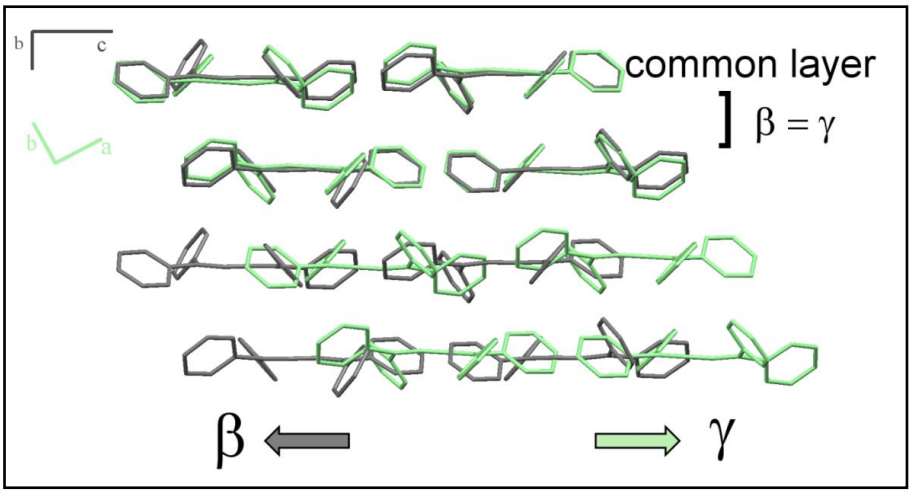

Figure 26 Comparison of the polymorph β - TPB and γ-TPB

δ- TPB

We have discovered a fourth phase, named δ, through a DSC analysis of the commercial product. The thermogram showed the presence of an unknown phase, now identified as δ polymorph, with melting point higher than α polymorph.

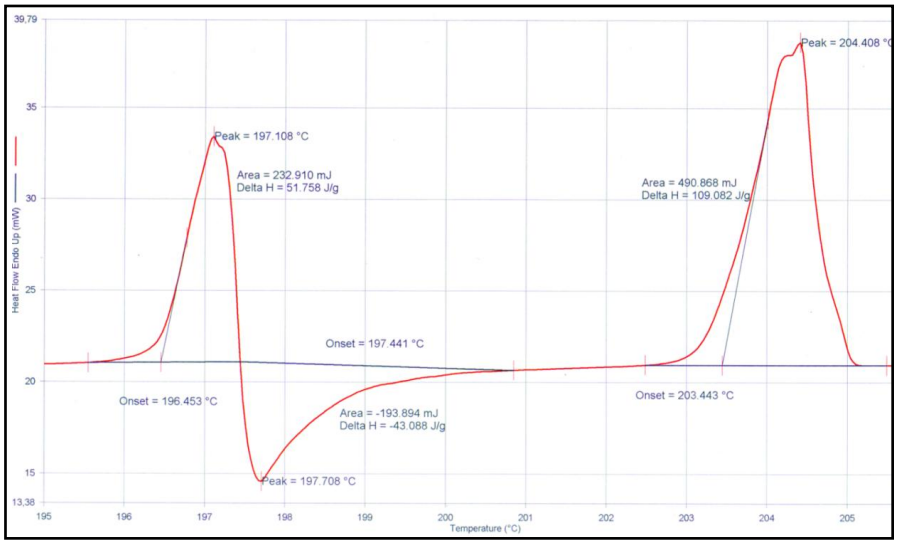

Figure 27 shows the DSC of the commercial product. First pick at 197,108 C represents the α-phase melted, the pick at 197,708 C shows the δ-phase recrystallized and the pick at 204,408 C represents the δ-phase melted

I have found that the δ polymorph can be obtained in another way: the α phase is heated up to its melting, then cooling the melt to a cooling rate higher than 0.5°C/min it is obtained the new polymorph is obtained.

The δ-TPB is triclinic, P-1, with three molecules per unit cell. The morphology is shown in Fig. 28.

Figure 28 shows the delta phase morphology

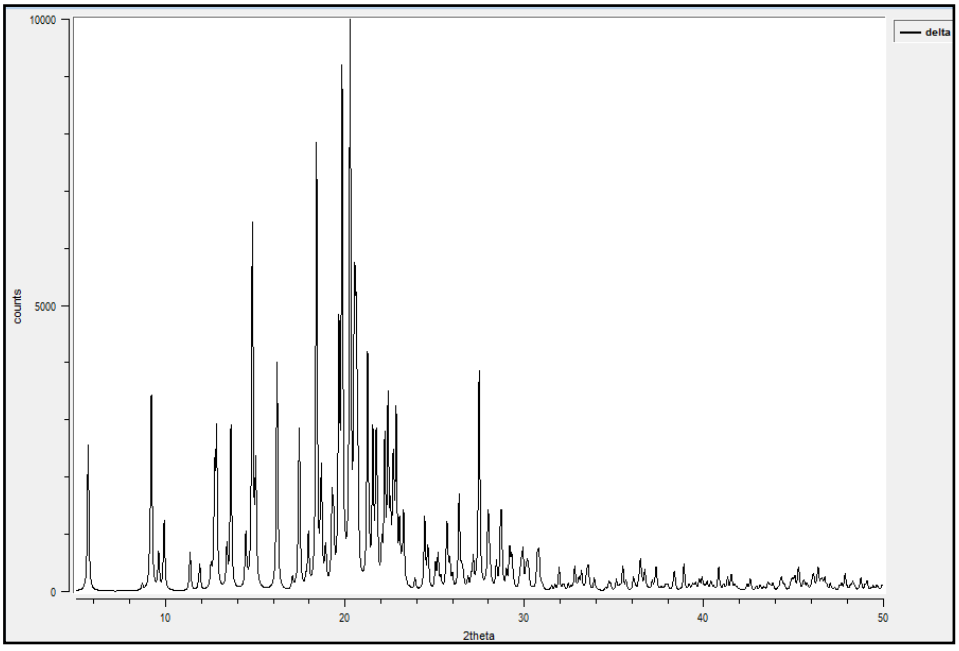

Figure 29 shows the powder pattern of delta phase

1.2 Molecular conformations

The TPB molecule presents different conformations in the various polymorphs, which as we have seen have also different packing. In the α polymorph the molecules have a conformation of approximate C_1 symmetry, and pack in a herringbone pattern. In the β and γ polymorphs the molecules have approximate C_2 conformation and crystallize arranging themselves in parallel to each other in a staggered manner. The packing of the molecules in the γ phase is indeed very similar to that present in the β phase: In both cases, the molecules have approximate C_2 symmetry and they are arranged with the butadiene skeleton parallel along the crystallographic c-axis[41]. From the thermodynamic point of view energy conformation C_2 is slightly favored (ΔE = 4.1681 kJ / mol).

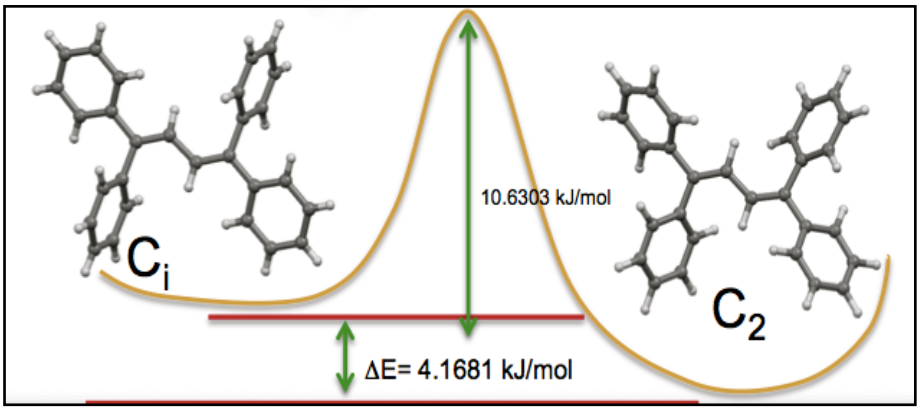

Figure 30 Conformations C_i and C_2 of the molecule of TPB and ΔE of relative conformations

In the new δ polymorph we have discovered, one molecule presents a C_i conformation as in the α-phase and two molecules have a C_2 conformation, and are arranges as in the the γ-phase (Figs. 31-33).

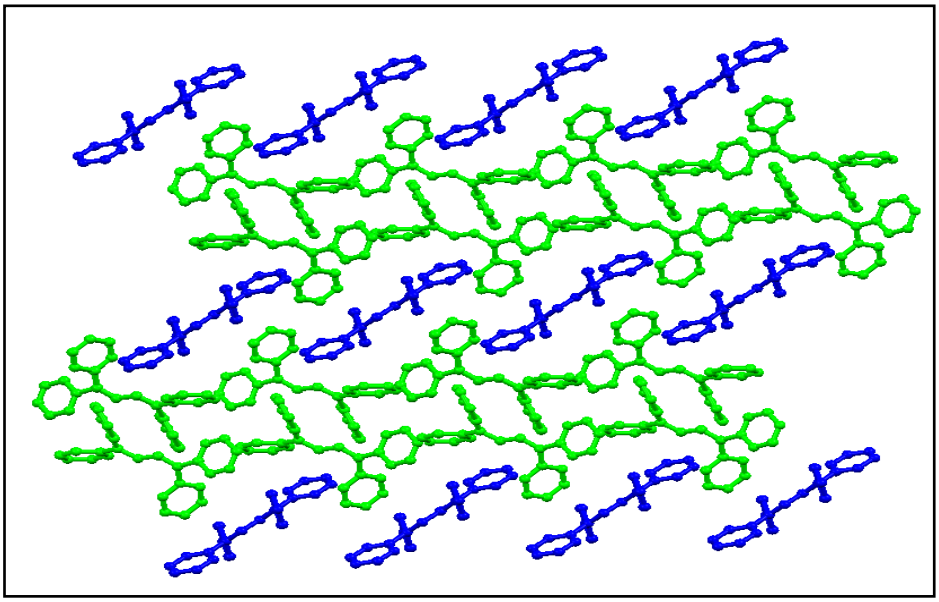

Figure 31 Packing in the δ-polymorph TPB highlighting the conformations C_i (blue) and C_2 (green)

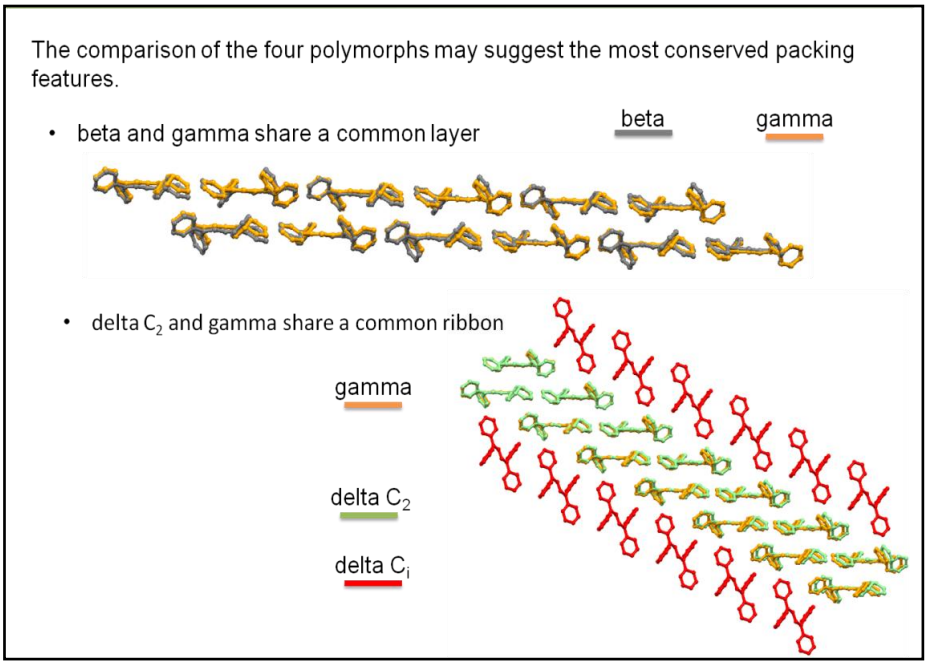

Figure 32 The comparison of polymorphs of TPB

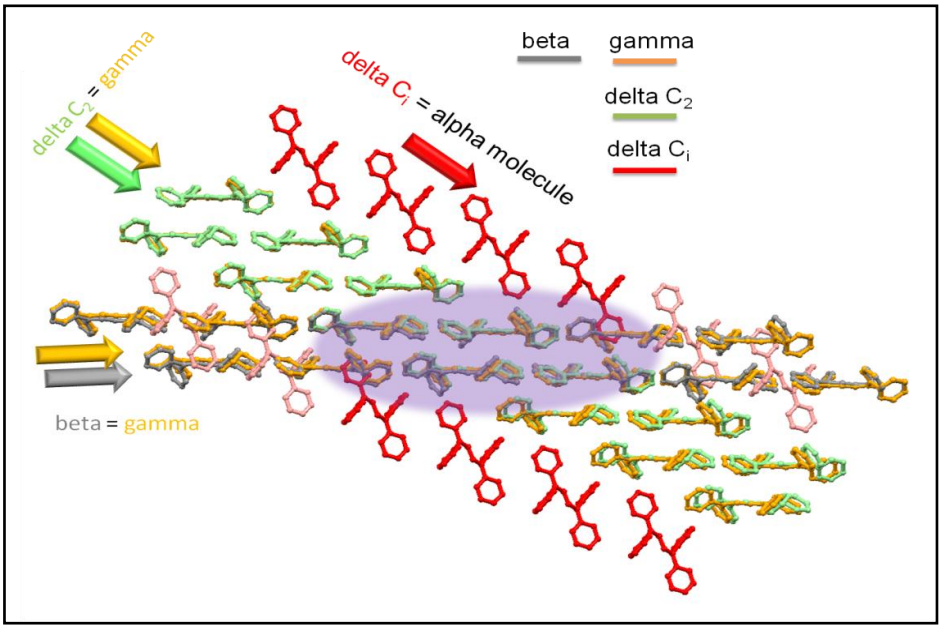

Figure 33 Delta is a peculiar mixture of packing and conformational possibilities

1.3 Experimental details

The α-form is the most commonly encountered polymorph and can be prepared by sublimation, melting followed by slow cooling or crystallization from a variety of solvents.

TPB was dissolved in ca. 4 mL of the respective solvent, filtered, and kept for slow evaporation at room temperature. Single crystals were obtained over a period of two days to a fortnight. The experimental procedure was the following: about 30 mg of TPB were dissolved in ca. 4 mL of solvent, filtered, and kept for slow evaporation at room temperature. Single crystals suitable for X-ray diffraction were obtained over a period of two days to a fortnight.

β-TPB can only be obtained by physical vapor transport method[42].

γ-TPB is non reproducibly obtained by crystallization from ethyl- or butyl-acetate, this polymorph is obtained with the same crystallization procedure of α-phase.

δ-TPB is obtained by melting α phase followed by cooling rate higher than 0.5°C/min.

Single crystal X-ray diffraction data were collected using the Mo Kα radiation (λ = 0.71073 Å) on a SMART APEX2 diffractometer; all data were collected at room temperature (293K). The collected intensities were corrected for Lorentz and polarization factors and empirically for absorption by using the SADABS program[40]. Structures were solved by direct methods using SIR97[41] and refined by full-matrix least-squares on

[40] a) SAINT: SAX, Area Detector Integration, Siemens Analytical instruments INC., Madison, Wisconsin, USA. b) SADABS: Siemens Area Detector Absorption Correction Software, G. Sheldrick, 1996, University of Goettingen, Germany

[41] Sir97: A new Program for Solving and Refining Crystal Structures, A. Altomare, M.C. Burla, M. Cavalli, G. Cascarano, C. Giacovazzo, A. Gagliardi, A.G. Moliterni, G. Polidori, R. Spagna, 1997, Istituto di Ricerca per lo Sviluppo di Metodologie Cristallografiche CNR, Bari

all F^2 using SHELXL97[42] implemented in the WinGX package[43]. Hydrogen atoms were introduced in calculated positions. Anisotropic displacement parameters were refined for all non-hydrogen atoms. Hydrogen bonds have been analyzed with SHELXL97[45] and PARST97[44] and extensive use was made of the Cambridge Crystallographic Data Centre packages[45] for the analysis of crystal packing. Table 1 summarizes crystal data and structure determination results of the, δ form, the new polymorph.

[42] Shelxl97. Program for structure refinement, G. Sheldrick, University of Goettingen, Germany, 1997
[43] L.J. Farrugia, J. Appl. Cryst., 1999, 32, 837–838
[44] M. Nardelli, J. Appl. Cryst., 1995, 28, 659
[45] a) F.H. Allen, O. Kennard, R. Taylor, Acc. Chem. Res., 1983, 16, 146–153; b) I. J. Bruno, J.C. Cole, P.R. Edgington, M. Kessler, C.F. Macrae, P. McCabe, J. Pearson, R. Taylor, ActaCrystallogr. 2002, B58, 389–397

Table 1 Crystal data and structure refinement of the δ form

	Delta form	
Empirical formula	$C_{28}H_{22}$	
Formula weight	358,74	
Temperature	293(2) K	
Wavelength	0.71073 Å	
Crystal system, space group	Triclinic, P-1	
Unit cell dimensions	a = 9.896(5) Å	α = 84.076(7)°
	b = 10.212(5) Å	β = 76.316(7)°
	c = 16.090(7) Å	γ = 88(75)°
Volume	1571.3(13) $Å^3$	
Z, Calculated density	3, 1.136Mg/m^3	
Absorption coefficient	0.118 mm^{-1}	
F(000)	570	
Crystal size	0.140	
Theta range for data collection	2.28° to 23.23°	
Limiting indices	$-9\leq h\leq 9$, $-9\leq k\leq 9$, $-11\leq l\leq 8$	
Completeness to theta	3458 / 1830 [R(int) = 0.0396]	
Refinement method	90.3%	
Data / restraints / parameters	Full-matrix least-squares on F^2	
Goodness-of-fit on F^2	1830 / 0 / 198	
Final R indices [I>2sigma(I)]	1.063	
R indices (all data)	R_1 = 0.0600, wR_2 = 0.1640 R_1 = 0.0927, wR_2 = 0.1878	
Largest diff. peak and hole	0.323 and -0.233 $e\cdot Å^{-3}$	

2. The solvated forms of TPB

During the thesis work, we have discovered a solvated form of TPB. Through a careful design we have achieved a particularly interesting solvated form containing cyclohexane as a guest. Most interestingly the guest is arranged in well ordered arrays inside channels throughout the crystal packing; the system is very unstable and looses cyclohexane in a few minutes after removal from the solution due to the fact that the channels are not able to trap the guest with a sufficient stability.
Another key result of this work is that when the solvate system is exposed to cyclohexanone vapors it does not decompose but exchanges cyclohexane with cyclohexanone without losing crystallinity. This shows that the channels are stabilized by the presence of cyclohexanone.

2.1. Crystallization from cyclohexane and loss of the solvent

TPB was purchased from Sigma-Aldrich and used as received. The experimental procedure was the following: about 30 mg of TPB were dissolved in ca. 4 mL in a saturated solution in cyclohexane, filtered, and kept for slow evaporation at room temperature. Single crystals suitable for X-ray diffraction were obtained over a period of two days. The X-ray analysis showed that the solvent is incorporated into a new crystalline structure.

Molecular structure an labelling of the solvated form are shown in Figure 34.

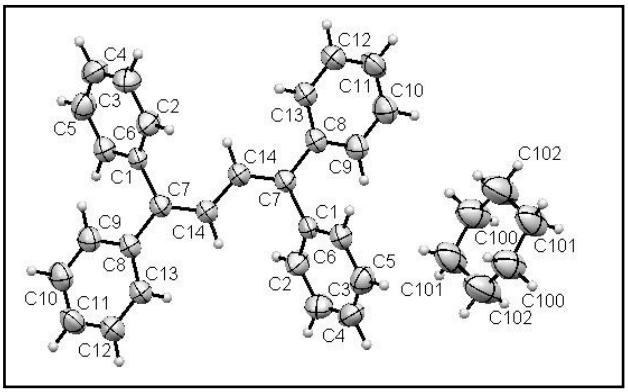

Figure 34 The solvated form of TPB

The cyclohexane solvated form of TPB crystallizes in a monoclinic P-1 space group.

In Fig. 35, 36, 37 I report the packing of the solvated form along the crystallographic axes a, b and c respectively.

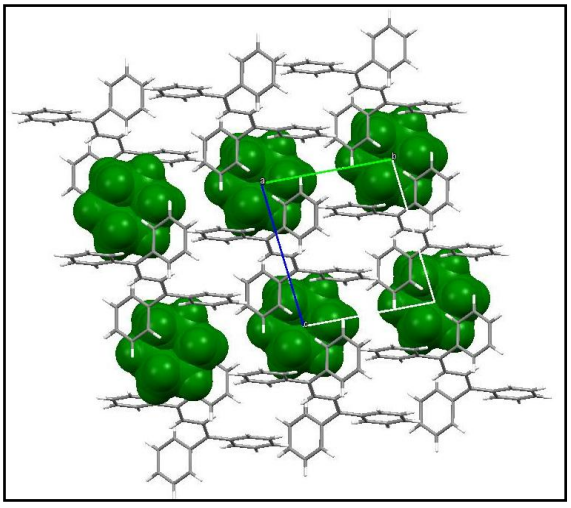

Figure 35 View along a

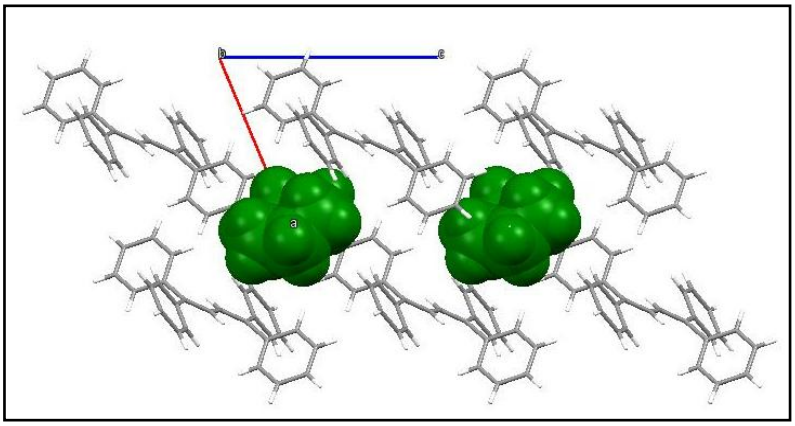

Figure 36 View along b

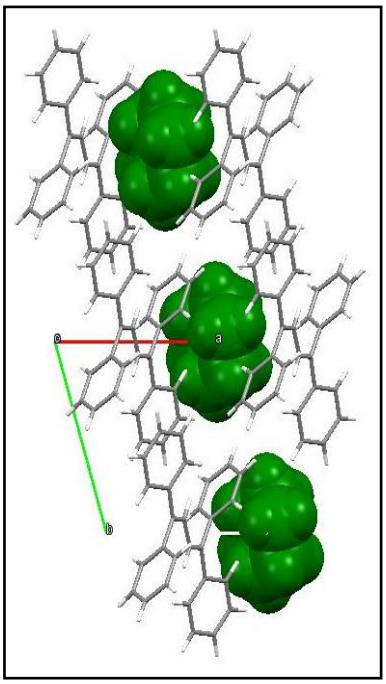

Figure 37 View along c

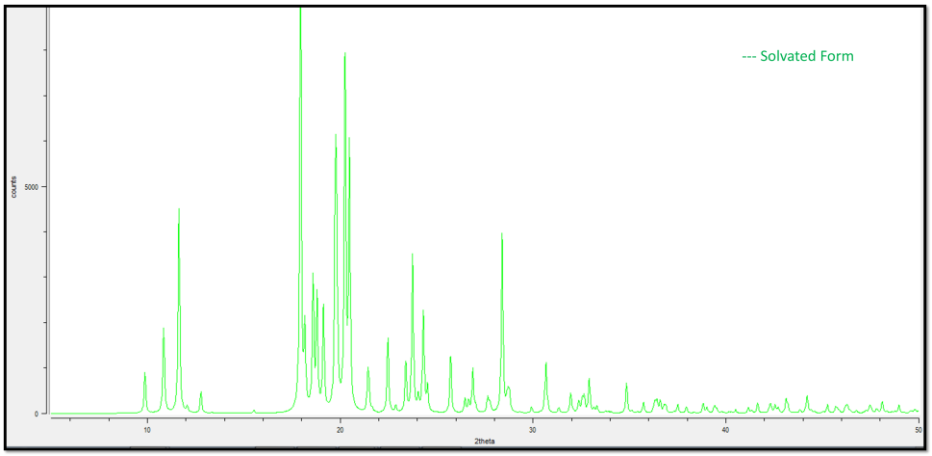

Figure 38 Powder pattern of the TPB-cycloexane

We have analyzed TPB-cyclohexane by TGA (Thermogravimetric analysis) and DSC (Differential scanning calorimetry), in fact, Fig. 39. shows that the guest leaves TPB very quickly at r.t, subsequently, TPB melts approximately at 200 C.

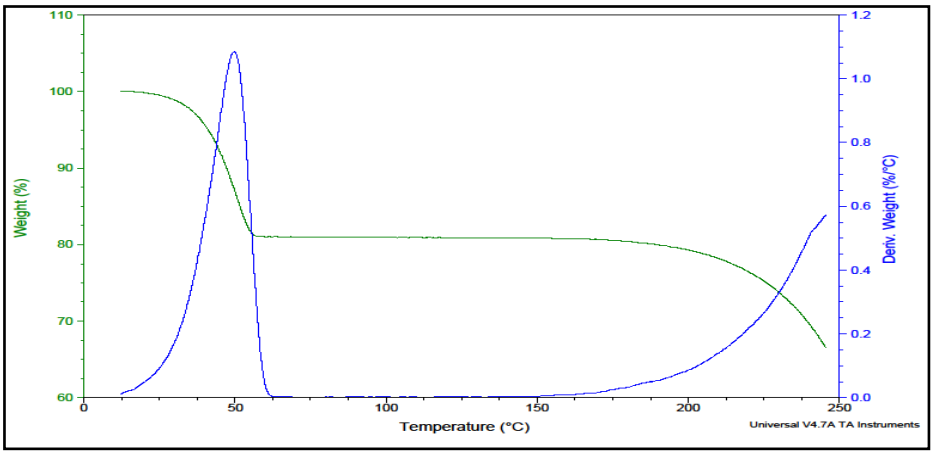

Figure 39 Thermogravimetric and Calorimetric Data of TPB-cyclohexane. Diagrams in blue and in green show the DSC and the TGA of the solvated phase, respectively. It is noted that at r.t there is the loss of the guest.

2.2. Guest exchange reaction

We have verified that the cyclohexane solvated form exchange with other guest vapours. Exchange reactions were performed by exposing TPB-cycloexane to the vapors of cyclohexanone. The experimental procedure was the following: about 30-40 mg of TPB-cyclohexane were introduced inside in a vial, this powder was exposed to vapors of cyclohexanone, the presence of the ketone was monitored by IR and powder pattern (Fig. 40).

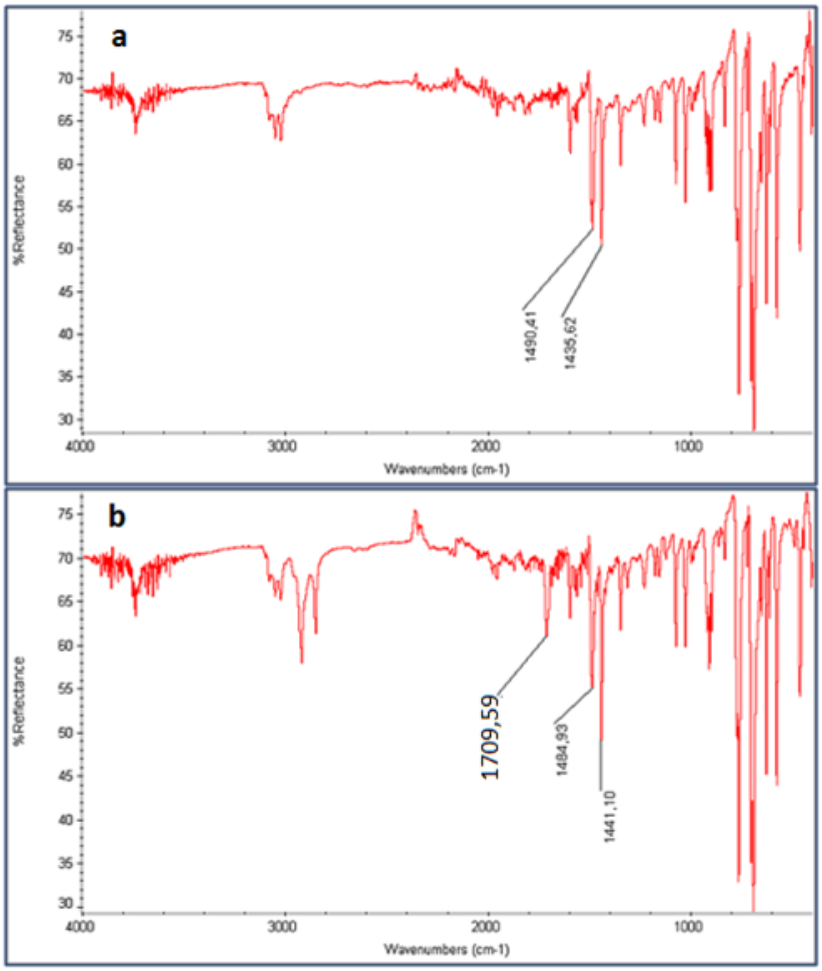

Figure 40 shows IR spectra of the TPB-cyclohexane (a), and the presence of cyclohexanone (b), Ketone peak is present at 1709.59 cm^{-1}

During our exploration of solid–vapor reactions as a means of forming the respective solvated form, polycrystalline powder was exposed to the vapour of cyclohexanone, and the extent of guest uptake was recorded gravimetrically as a function of time (Figure 41). Sorption of the guest occurred slowly in air, but the rate of uptake was significantly enhanced when the reaction chamber was evacuated prior to admitting the vapor.

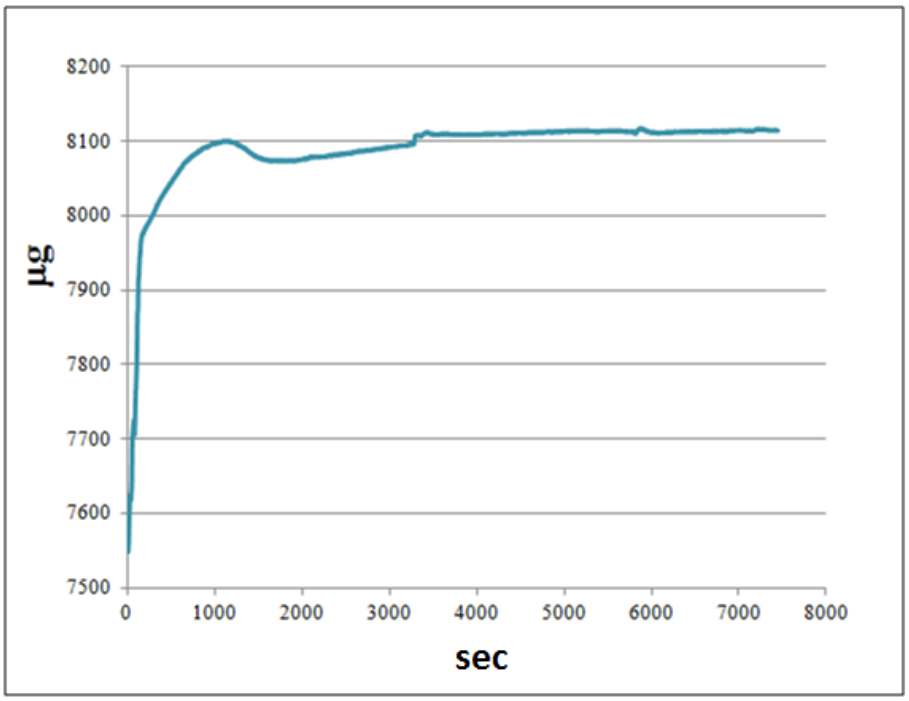

Figure 41 Sorption kinetics (recorded at r.t.) showing extent of reaction a as a function of time for the uptake of cyclohexanone

We have also verified that the cyclohexanone, like the cyclohexane, does not remain inside the system. IR spectra in Figure 42 shows the constant loss of cyclohexanone.

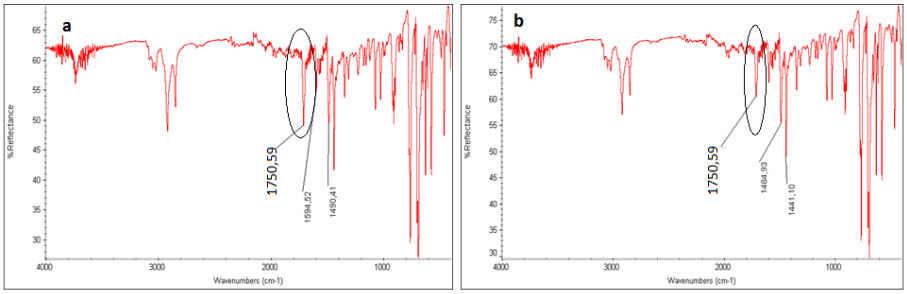

Figure 42 shows the pick of cyclohexanone at t=0 (a) that decrease next 20 minutes (b) from the exposition at the normal atmosphere

Solid-vapor sorption reactions at r.t. were monitored using a microbalance that was constructed in the laboratories of the prof. Leonard Barbour at the University of Stellenbosch (South Africa).

Solvated TPB were weighed on a microbalance under vacuum at r.t., 1 ml of cyclohexanone was injected into the microbalance and the weight at the beginning was 8,73 mg, the minimum point was 7,55 mg and the maximum point (when the system adsorbs cyclohexanone) was 8,10 mg Fig.41.

2.3. Desolvated Phase

TPB-cyclohexane loose the guest after few minutes at r.t., after one week, the powder is the alpha phase, however, after 3 days, the powder is an intermediate phase that present difference respect at the other polymorphs (Fig 43)

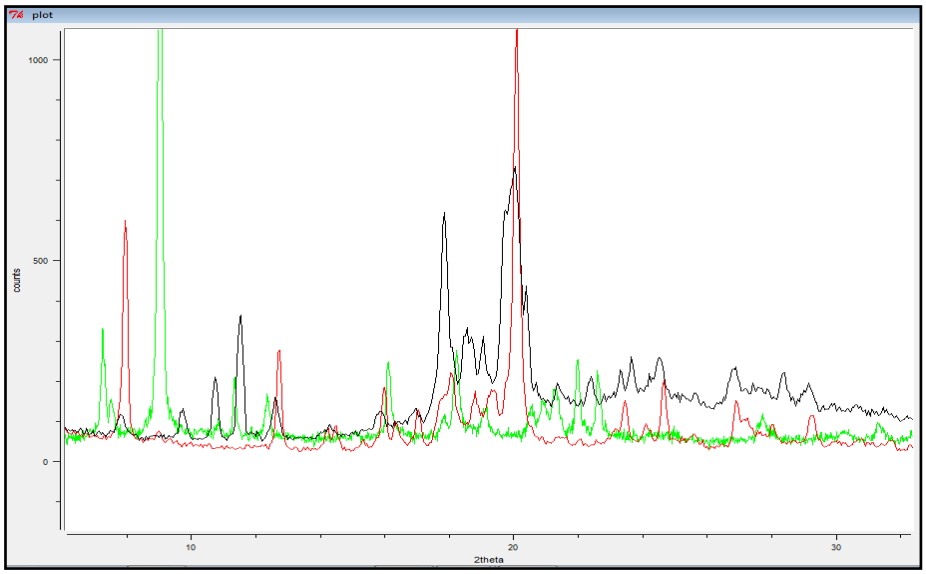

Figure 43 The different spectra of TPB solvated. Solvated phase at t=0 (black), intermediate form after 3 days (green), TPB solvated after one week (red)

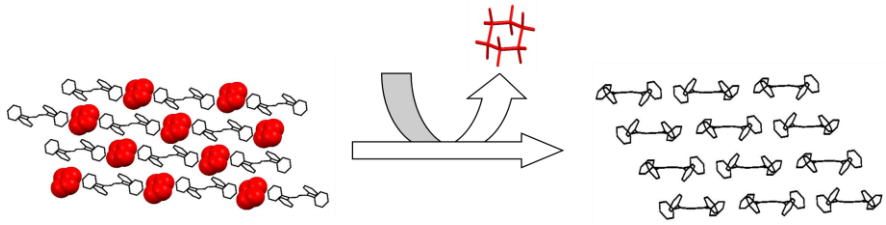

Figure 44 After one week the solvated form becomes alpha phase

2.4. Experimental details

TPB was purchased from Sigma-Aldrich an used as received. Single crystal X-ray diffraction data were collected using the Mo Kα radiation (λ = 0.71073 Å) on a SMART APEX2 diffractometer; all data were collected at room temperature (293K). The collected intensities were corrected for Lorentz and polarization factors and empirically for absorption by using the SADABS program[43]. Structures were solved by direct methods using SIR97[44] and refined by full-matrix least-squares on all F^2 using SHELXL97[45] implemented in the WinGX package[46]. Hydrogen atoms were introduced in calculated positions. Anisotropic displacement parameters were refined for all non-hydrogen atoms. Hydrogen bonds have been analyzed with SHELXL97[45] and PARST97[47] and extensive use was made of the Cambridge Crystallographic Data Centre packages[48] for the analysis of crystal packing. Table 2 summarizes crystal data and structure determination results.

Table 2 Crystal data and structure refinement of TPB solvated form

	Solvated form	
Empirical formula	C_{34} H_{34}	
Formula weight	445,74	
Temperature	293(2) K	
Wavelength	0.71073 Å	
Crystal system, space group	monoclinic, P-1	
Unit cell dimensions	a = 8.846(3) Å	α = 74.927(6)°
	b = 8.839(3) Å	β = 64.092(5)°
	c = 10.016(3) Å	γ = 68.128(6)°
Volume	649.3 (4) $Å^3$	
Z, Calculated density	1, 0.917Mg/m^3	
Absorption coefficient	0.118 mm^{-1}	
F(000)	190	
Crystal size	0.140	
Theta range for data collection	2.28° to 23.23°	
Limiting indices	$-9\leq h\leq 9$, $-9\leq k\leq 9$, $-11\leq l\leq 8$	
Completeness to theta	3458 / 1830 [R(int) = 0.0396]	
Refinement method	98.9 %	
Data / restraints / parameters	Full-matrix least-squares on F^2	
Goodness-of-fit on F^2	1830 / 0 / 198	
Final R indices [I>2sigma(I)]	1.063	
R indices (all data)	R_1 = 0.0600, wR_2 = 0.1640 R_1 = 0.0927, wR_2 = 0.1878	
Largest diff. peak and hole	0.323 and -0.233 $e\cdot Å^{-3}$	

3. The study of the TPB behavior by gel crystallization

3.1. Introduction

Gels are materials consisting of a three-dimensional network that spans the volume of a liquid medium and ensnares it through surface tension effects. Gels are defined as a substantially diluted cross-linked system, which exhibits no flow when in the steady state.

Both by weight and volume gels are mostly fluid in composition and thus exhibit densities similar to those of their constituent liquids[46].

Supramolecular gels are those held together by non covalent interactions such as hydrogen bonds and metal-ligand interactions. Crystallization of a gelator compound is not an easy job, the examples available in the literature are very few, in particular when small coordination compounds are involved[47]. Steed, Clarke and coworkers have very recently published an exhaustive review on metal- and anionbinding supramolecular gels[48]. Of particular interest are supergelator systems, because they are effective in gel formation at very low concentration, i.e. below 1% w/v)[56].

Gels find applications in almost all areas of materials chemistry[49] and are nowadays been approached with the objective of finding materials suitable for crystallization of new crystal phases[50]. The quest for new crystal forms of molecular species is very important because of the number of potential applications of the different physico-chemical properties of different

[46] (a) R. G. Weiss and P. Terech, *Molecular Gels Materials with Self-Assembled Fibrillar* Networks, Springer, Dordrecht, 2006; (b) D. K. Smith, in *Organic Nanostructures*, ed. J. L. Atwood and J. W. Steed, WILEY-VCH, Weinheim, 2008, pp. 111–148

[47] (a) M. M. Piepenbrock, N. Clarke and J. W. Steed, *Langmuir*, 2009, **25**, 8451–8456; (b) N. N. Adarsh, P. Sahoo and P. Dastidar, *Cryst. Growth Des.*, 2010, **10**, 4976–4986

[48] M. M. Piepenbrock, G. O. Lloyd, N. Clarke and J. W. Steed, *Chem. Rev.*, 2010, **110**, 1960–2004

[49] A. R. Hirst, B. Escuder, J. F. Miravet and D. K. Smith, *Angew. Chem., Int. Ed.*, 2008, **47**, 8002–8018

[50] J. A. Foster, M. M. Piepenbrock, G. O. Lloyd, N. Clarke, J. A. K. Howard and J. W. Steed, *Nat. Chem.*, 2010, **2**, 1037–1043

crystal forms of a same species (polymorphs, co-crystals, hydrates, solvates, salts etc.)[60,51].

Classification of gels

Gels can be classified in different ways based upon their origin constitution, type of crosslinking and medium (scheme 1).

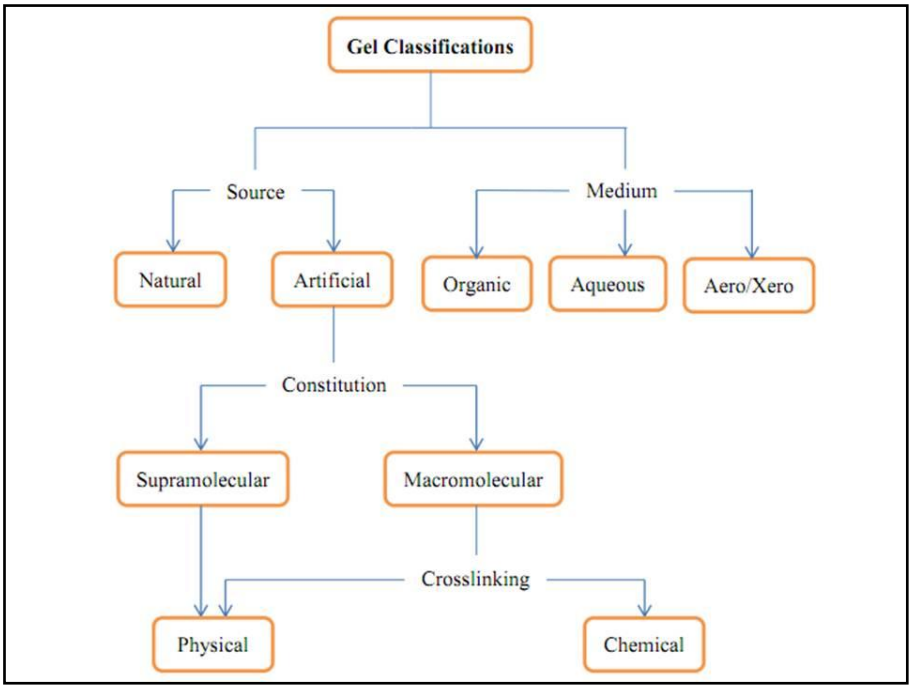

Scheme 1. Classification of gels. Gels can be organized according to multiple characteristics: source of the gel (natural/artificial), gel medium (organic/aqueous/aero/xero), constitution of the gel (macromolecular/supramolecular), and type of crosslinking (physical/chemical).

[51] (a) D. Braga, F. Grepioni and L. Maini, *Chem. Commun.*, 2010, **46**, 6232–6242; (b) J. Bernstein, *Polymorphism in Molecular Crystals*, Clarendon Press, Oxford, 2002; (c) U. Griesser, *Polymorphism in the Pharmaceutical Industry*, ed. R. Hilfiker, Wiley VCH, Weinheim, 2006, pp. 211–234; (d) S. L. Childs and M. J. Zaworotko, *Cryst. Growth Des.*, 2009, **9**, 4208–4211; (e) G. R. Desiraju, *Cryst. Growth Des.*, 2008, **8**, 3–5

Gels can be classified into natural gels and artificial or synthetic gels. Gels derived from synthetic compounds can be subdivided into macromolecular (polymer) and molecular gels based on their constitution. Macromolecular gels can be formed either by chemical cross-linking or physical interactions. When gels are formed by strong chemical bonds, they cannot be redissolved and their formation is thermally irreversible, instead gels obtained by weak noncovalent interactions are formed in a reversible way.
Depending upon the solvents, gels can be classified into organogels and hydrogels. If the gel is formed with organic solvents it is called organogel, if it is formed with water it is called hydrogel. Depending upon the drying process, xerogels or aerogels can be obtained.
Gels derived from low molecular mass compounds are called supramolecular gels. In recent years low molecular mass gelators (LMWGs) have attracted considerable interest due to molecules of great structural diversity. Their discovery and development are particularly important, as potential applications can be envisaged in almost all areas of materials chemistry[59].

Gelation mechanism and formation of supramolecular gels

The formation of gels from small organic molecules or complexes is an excellent example of a hierarchical supramolecular self-assembly process[57,60]. The aggregation of gelator molecules is driven by multiple, weak interactions such as hydrogen bonding interactions, π-πstacking, metal coordination[57], van der Waals interactions[57]. The phenomenon of gelation is presumably due to formation of nano- to micrometer-sized fibers becoming entangled and trapping solvent via surface tension.

To understand the mechanism of gel formation, a gel can be broken down into a primary, secondary, and tertiary structure, much like a protein (Figure 45)[52,53].

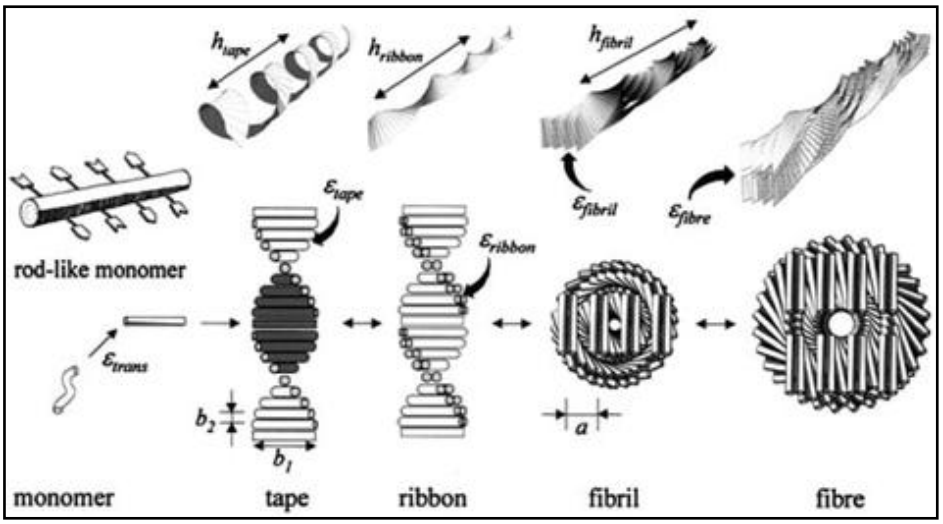

Figure 45 Hierarchical self-assembly process of gel-phase materials. As illustrated for synthetic systems developed by Aggeli and coworkers[54]

The primary structure (angstrom to nanometer scale) is determined by the molecular level recognition events that promote anisotropic aggregation in one or two dimensions of the gelator molecules. To achieve gelation, there must be a balance between the tendency of the molecules to dissolve and to aggregate.

The secondary structure (nano- to micrometer scale) is defined as the morphology of the aggregates, that is micelles, vesicles, fibers, ribbons or sheets, and is directly influenced by the molecular structure[65,66].

[52] G. C. Maity, *Journal of Physical Sciences*, 2007, **11**, 156-171
[53] P. J. Flory, *Faraday Discuss*. 1974, ***57***, 7
[54] P. Jonkheijm, P. van der Schoot, A.P.H.J. Schenning and E. W. Meijer, *Science*, 2006, **313**, 80–83

Finally, the tertiary structure of a gel (micro- to millimeter scale) involves the interaction of individual aggregates and ultimately determines whether a gel is formed or, instead, fibers precipitate in solution.

Gels derived from small molecules are usually prepared by heating the compounds in the appropriate solvent and cooling the resulting saturated solution to room temperature. When the hot solution is cooled, molecules start to condense and three are the possible outcomes:

(a) a highly ordered aggregation giving rise to crystals;

(b) a random aggregation resulting in an amorphous precipitate;

(c) an aggregation process intermediate between these two that gives rise to a gel.

3.2. Polymorphs from gels

I have studied the polymorphism of TPB in Poly(ethylene oxide) (PEO), it is one of the most studied water-soluble synthetic polymers[55]. Owing to its biocompatibility[56], PEO is used as a model for biomedical applications, e.g. in drug-delivery systems[57]. PEO is soluble in water over a wide range of degrees of polymerization and at moderate temperatures (298–333 K), and it can be prepared as a hydrogel with a pore diameter of around 3-20 mm[58]. The use of PEO as a gel has been reported for the crystallization of extended inorganic solids[59], one organic molecule[60], some coordination

[55] Allen, F. H. (2002). Acta Cryst. B58, 380–388. Bailey, F. E. Jr & Koleske, J. V. (1976). Poly(ethylene oxide). New York: Academic Press

[56] Bianconi, P. A., Lin, J. & Strzelecki, A. R. (1991). Nature (London), 349, 315–317. Blank, Z. & Reimschuessel, A. C. (1974). J. Mater. Sci. 9, 1815–1822. Bruker (2010). APEX2. Version 2010.1. Bruker AXS Inc., Madison, Wisconsin, USA

[57] Carlucci, L., Ciani, G., Garcı´a Ruiz, J. M., Moret, M., Proserpio, D. M. & Rizzato, S. (2009). Cryst. Growth Des. 9, 5024–5034. Chandrasekhar, R. (2000). J. Mater. Sci. Lett. 19, 1801–1803. Dhawan, S., Dhawan, K., Varma, M. & Sinha, V. R. (2005). Pharm. Technol. 29, 82–95

[58] Emami, S. H. (2008). Polyethylene Oxide Hydrogels: Synthesis and Characterization. Saarbru¨ cken: VDM Verlag Dr Mu¨ ller. Garcı´a-Ruiz, J. M. (1986). J. Cryst. Growth, 75, 441–453

[59] Garcìa-Ruiz, J. M., Herna´ndez-Herna´ndez, M. A. & Go´ mez-Morales, J. (2005). Industrial Crystallization, VDI Berichte, Vol. 1901, pp. 963–968. Du¨ sseldorf: VDI

[60] Garcia-Ruiz, J. M., Novella, M. L., Moreno, R. & Gavira, J. A. (2001). J. Cryst. Growth, 232, 165–172. Garcı´a-Ruiz, J. M. & Ota´ lora, F. (2004). Crystal Growth – From Fundamentals to Technology, edited by G. Mu¨ ller, J.-J. Me´ tois & P. Rudolph, pp. 369–386. Amsterdam: Elsevier

polymers[61] and, recently, proteins[62]. These PEO gels were obtained using a variety of solvents, including water[63], dichloromethane[64], dichloroethane[65], acetonitrile[66] and some of their mixtures[67], but there is still only limited information available on the proper procedure for the preparation of PEO gels, as well as on the feasibility of using PEO to form gels with a comprehensive list of organic solvents.

PEO gel has been utilized because TPB is insoluble in water, in this work I report different kind of crystallizations of TPB in PEO.

[61] Go´ mez-Morales, J., Herna´ndez-Herna´ndez, A., Sazaki, G. & Garcı´a- Ruiz, J. M. (2010). Cryst. Growth Des. 10, 963–969. Hammouda, B., Ho, D. L. & Kline, S. (2004). Macromolecules, 37, 6932–6937. Henisch, H. K. (1970). Crystal Growth in Gels, 2nd ed. New York: Dover Publications Inc

[62] Jimenez-Lo´ pez, C., Rodrı´guez-Navarro, A., Domı´nguez-Vera, J. M. & Garcı´a-Ruiz, J. M. (2003). Geochim. Cosmochim. Acta, 67, 1667– 1676. Lide, D. R. (2004). Editor. Handbook of Chemistry and Physics. Boca Raton: CRC Press. Nardin, G., Randaccio, L., Bonomo, R. P. & Rizzarelli, E. (1980). J. Chem. Soc. Dalton Trans. pp. 369 375

[63] Pauchet, M., Morelli, T., Coste, S., Malandain, J.-J. & Coquerel, C. (2006). Cryst. Growth Des. 8, 1881–1889

[64] Pietras, Z., Lin, H.-T., Surade, S., Luisi, B., Slattery, O., Pos, K. M. & Moreno, A. (2010). J. Appl. Cryst. 43, 58–63. Reddy, C. M., Basavoju, S. & Desiraju, G. R. (2005). Chem. Commun. pp. 2439–2441. Robert, M. C. & Lefaucheux, F. (1988). J. Cryst. Growth, 90, 358–367

[65] Robert, M. C., Vidal, O., Garcı´a-Ruiz, J. M. & Ota´ lora, F. (1999). Crystallization of Nucleic Acids and Proteins: A Practical Approach, edited by A. Ducruix & R. Giege´, pp. 149–175. New York: Oxford University Press

[66] Roma´n-Alpiste, M. J., Martı´n-Ramos, J. D., Castin˜ eiras-Campos, A., Bugella-Altamirano, E., Sicilia-Zafra, A. G., Gonza´lez-Pe´ rez, J. M. & Niclo´ s-Gutie´ rrez, J. (1999). Polyhedron, 18, 3341–3351. Sheldrick, G. M. (2008). Acta Cryst. A64, 112–122. Yaghi, O. M., Li, G. & Li, H. (1997). Chem. Mater. 9, 1074–1076

[67] Zhang, S.-S., Niu, S.-Y., Jie, G.-F., Li, X.-M., Xu, H., Shi, X. & Jiao, K.(2006). Chin. J. Chem. 24, 51–58

Table 3 Solvents used in this work

Solvent	Acronym	Boiling point (K)
Toluene	TOL	383.78
Nitromethane	NME	374.34
Water	H2O	373.15
Heptane	HEP	371.55
Acetonitrile	ACN	354.80
2-Propanol	ISP	355.45
1,2-Dichloroethane	DCE	356.65
Benzene	BZN	353.24
Butanone	BNA	352.71
Ethanol	EOH	351.44
Ethyl Acetate	ETA	350.56
n-Hexane	HEX	341.88
Ciclhoexane	CHEX	354,00
Methanolo	MET	337.75
Tetrahyidrofuran	THF	338.15
Chloroform	CLF	334.32
Acetone	ACE	329.20
Dichloromehtane	DCM	313.15
n-Pentane	PEN	309.21

3.3. Crystallization techniques

Once the PEO-compatible solvents had been identified, the feasibility of using these new gels as crystal-growth media was evaluated. For this purpose, the following crystallization techniques were explored with prof. Silvia Rizzato of the University of Milan.

Solvent evaporation

Different crystallization experiments were performed using the gels obtained with PEO compatible solvents of the compound to be crystallized. In general, a typical experiment (Fig. 46a) required the preparation of a solution of the compound at a given concentration in a screw-capped 2 ml glass vial, and then the addition of the PEO powder whilst stirring the solution. At the end, the tube was covered with a plastic cap and the solution left to gel undisturbed at 298 K during solvent evaporation.

Antisolvent liquid diffusion.

Antisolvent crystallization experiments were carried out by preparing PEO gels with solvents in which the compounds to be crystallized had been shown to be soluble. Once gelled, the antisolvent was carefully poured onto the gel. A typical experiment (Fig. 46b) began with the preparation of 1 ml of PEO gel with an organic solution of the studied compound in a screw-capped 2 ml glass vial. Once the gel had been obtained, 0.5 ml of antisolvent was layered over the gel.

Finally, the system was covered with a plastic cap and left undisturbed at 298 K. Antisolvent selection was based on two criteria: the antisolvent

must be miscible with the solvent, and the compound must be relatively insoluble in the antisolvent.

Counterdiffusion

Counterdiffusion crystallization experiments were carried out using glass U tubes. A typical experiment (Fig. 46c) started by closing the ends of the horizontal arm of the U tube with rubber septa, and then filling it with the PEO solution. Once a homogeneous gel had been obtained, the solutions of the reactants were carefully poured into the vertical arms of the U tube.

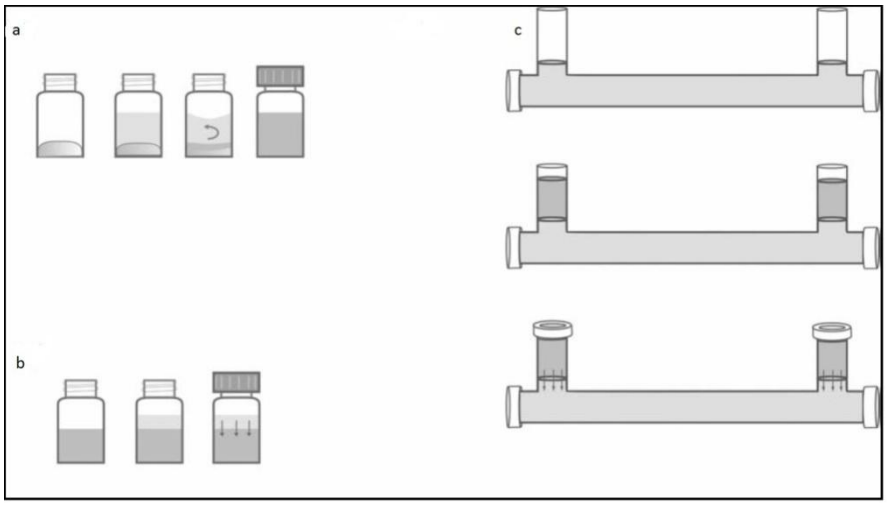

Figure 45 The experimental setup for the crystallization techniques used in this work. (a) Preparation of PEO gel or solvent-evaporation experiment when the studied compound is incorporated in the solution. (b) Addition of an antisolvent on top of a PEO

3.4.Crystallization from PEO doped gel

In this experiment was prepared a supersaturated solution of TPB in 1mL of the chosen solvent (see tab.4); this solution was microfiltered in a vial and 50 mg of PEO were added to it under stirring. The solution was allowed to stand in a closed vial.

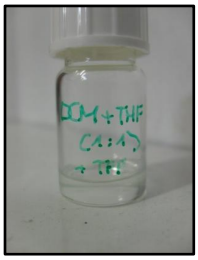

Gel doped

Table 4 G indicates the formation of the gel, F indicates the formation of the floccules and I that the PEO is insoluble; whereas r.t indicates that the experiments were conducted at room temperature (See tab. 1)

SOLVENTS	TEMPERATURE	CRYSTALLIZZATION TIME	OBSERVATIONS
DCM	r.t.	Around 3 days Morfology: needles α phase	G
ACN	r.t.	Around 45 days Morfology: prismatic α phase	G
NME	r.t.	Around 3 days Morfology: needles α phase	G
CLF	r.t.	Around 20 days Morfology: needles α phase	G

Figure 46 Crystal of α-TPB obtained in CLF

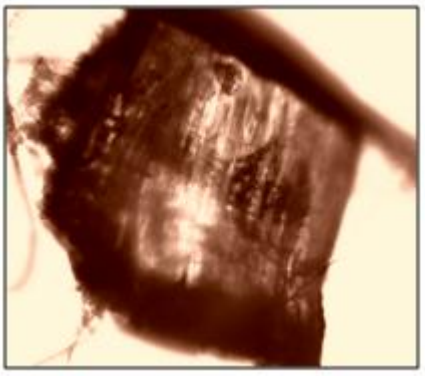

Figure 47 Crystal of α-TPB obtained in ACN

Procedure A: Crystallization obtained from mixtures of solvents from PEO doped gel in different proportions

In this experiment was prepared a supersaturated solution of TPB was prepared in 1 mL of the binary mixture indicated in Table 5. The solution was microfiltered in a vial; to it 50 mg of PEO were added, under stirring. The solution was then allowed to stand in a closed vial.

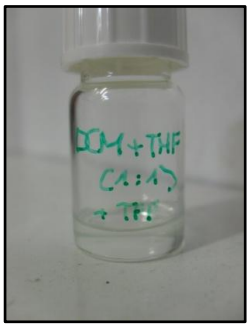

Gel in different proportions

Table 5 G indicates the formation of the gel, F indicates the formation of the floccules and I that the PEO is insoluble; whereas r.t. indicates that the experiments were conducted at room temperature (See tab. 1)

SOLVENTS	TEMPERATURE	CRYSTALLIZZATION TIME	OBSERVATIONS
DCM/EOH (1:1)	r.t.		F
DCM/EOH (4:1)	r.t.		F
DCM/EOH (1:4)	r.t.	Around 3 days Morfology: needles α phase.	F

Procedure B. Crystallization obtained from mixtures of solvents from doped PEO gel in different proportions

Initially, TPB was solubilised in DCM to obtain a supersaturated solution, then it was microfiltered in a vial containing the other solvent (see table 6). Then 50 mg of PEO were added to the binary mixture under stirring. In some cases the dissolution has not occurred, and then the mixture was heated until dissolution was observed. The solution was then closed and allowed to stand.

Table 6 G indicates the formation of the gel, F indicates the formation of the floccules and I that the PEO is insoluble; whereas r.t indicates that the experiments were conducted at room temperature (See tab. 1)

SOLVENTS	TEMPERATURE	CRYSTALLIZZATION TIME	OBSERVATIONS
DCM/THF (1:1)	r.t.	-	G
DCM/THF (4:1)	r.t.	-	G
DCM/THF (1:4)	r.t.	-	F
DCM/BNA (1:1)	313 K	Around 4 hours Morfology: needles α phase.	G
DCM/ETA (1:1)	r.t.	-	F
DCM/MET (1:1)	r.t.	-	F
DCM/ISP (1:1)	r.t.	-	G
DCM/TOL (1:1)	r.t.	-	G

3.5. Crystallization versus diffusion

Crystallizations were carried out in a glass container called "U-tube" (Fig. 49).

A not doped gel was prepared in DCM and inserted it in the middle section of the tube, a saturated solution of TPB was added in the chosen solvent on the one hand and on the other the anti-solvent (see table 7). Anti-solvent choice is focused on two points: anti-solvent must be miscible with solvent and TPB must be relatively insoluble in the anti-solvent.

Figure 48 U-tube

Table 7 G indicates the formation of the gel, F indicates the formation of the floccules and I that the PEO is insoluble; whereas r.t indicates that the experiments were conducted at room temperature (See tab. 1)

SOLVENT/ANTISOLVENT	TEMPERATURE	CRYSTALLIZZATION TIME	OBSERVATION
DCM/hexane	r.t.	Around 20 gg Morfology: needles α phase.	G
DCM/ISP	r.t.	Around 20 gg Morfology: needles α phase.	G

4. Conclusion

In this work, we have determined the conditions for obtaining four polymorphs and a solvated phase of TPB. The α and the δ ~~delta~~ phase can be obtained in a reproducible way, while the β and the γ -phases are elusive forms. From experimental results, the α phase is the most stable thermodynamically, while the δ phase is obtained under kinetic control.

Moreover, we have demonstrated a particular case of solvated form of TPB, where the host form interesting interactions only with cyclohexane, but the cyclohexane leaves the TPB very quickly. However, TPB-cyclohexane exchange with vapours of cyclohexanone, but also in this case the guest leaves very fast the host. After one week the desolvated powder is the α phase but after three days we have an intermediated form that present differences with the other phases. This is an interesting case of polymorphism of a organic molecule. It is really amazing how a molecule consisting of 28 carbon atoms sp^2 hybridized can give four different phases and a solvated form.

We have shown, with the fundamental contribution of the Prof. Silvia Rizzato, that poly (ethylene) oxide (PEO) can form gels with different organic solvents, this it is very important because TPB is insoluble in water and it is impossible to crystallize this compound in aqueous gels, such as agarose and sepharose. However, by different techniques such as the counterdiffusion method and gel doped we have obtained crystals of α-phase of size larger than the crystals obtained in solutions.

PART II: Gas sorption and separation

Studies of porous crystalline materials have almost exclusively been concerned with the zeolites for a relatively long time[68]. However, over the last decade these studies have evolved to include organic compounds[69,70,71,72,73,74] and coordination polymers[75,76,77,78,79]. The many applications associated with porous materials include catalysis[80], molecular storage[81,82,83,84,85,] molecular separation[83,86], molecular sensing[87], electronics[88,89], and ion exchange[90]. This chapter is mainly concerned with the storage and separation of gases. Nitrogen, carbon dioxide, methane, oxygen and hydrogen are the most commonly

[68] D. W. Breck in *Zeolite Molecular Sieves*, Wiley and Sons, New York, **1974**
[69] J. L. Atwood, L. J. Barbour & A. Jerga, *Science*, **2002**, *296*, 2367
[70] L. J. Barbour, *Chem. Commun.*, **2006**, 1163 and references therein
[71] J. L. Atwood, L. J. Barbour & A. Jerga, *Angew. Chem. Int. Ed.*, **2004**, *43*, 2948
[72] P. K. Thallapally, G. O. Lloyd, T.B. Wirsig, M.W. Bredenkamp, J. L. Atwood and L. J. Barbour, *Chem. Commun.*, **2005**, 5272
[73] A. P. Côté, A. I. Benin, N. W. Ockwig, M. O'Keeffe, A. J. Matzger & O. M. Yaghi, *Science*, **2005**, *310*, 1166
[74] P. K. Thallapally, T. B. Wirsig, L. J. Barbour & J. L. Atwood, *Chem. Commun.*, **2005**
[75] O. M. Yaghi, M. O'Keefe, N. W. Ockwig, H. K. Chae, M. Eddaoudi & J. Kim, *Nature*, **2003**, *423*, 705
[76] G. Férey, *Chem. Mater.*, **2001**, *13*, 3084
[77] A. J. Fletcher, K. M. Thomas & M. J. Rosseinsky, *J. Solid State Chem.*, **2005**, *178*, 2491
[78] J. L. C. Rowsell & O. M. Yaghi, *Angew. Chem. Int. Ed.*, **2005**, *44*, 4670
[79] T. Düren, L. Sarkisov, O. M. Yaghi, & R. Q. Snurr, *Langmuir*, **2004**, *20*, 2683
[80] T. Uemura, R. Kitaura, Y. Ohta, M. Nagaoka & S. Kitagawa, *Angew. Chem. Int. Ed.*, **2006**, *45*, 4112
[81] P. Finocchiaro & S. Failla in *Comprehensive Supramolecular Chemistry*, ed. J. L. Atwood, J. E. D. Davies, D. D. MacNicol and F. Vögtle, Elsevier Science, Oxford, **1996**, vol. 6
[82] J. Szejtli & T. Osa in *Comprehensive Supramolecular Chemistry*, ed. J. L. Atwood, J. E. D. Davies, D. D. MacNicol and F. Vögtle, Elsevier Science, Oxford, **1996**, vol. 3
[83] *Cyclodextrins* in *Comprehensive Supramolecular Chemistry*, ed. J. L. Atwood, J. E. D. Davies, D. D. MacNicol and F. Vögtle, Elsevier Science, Oxford, **1996**, vol. 3
[84] G. Férey, C. Mellot-Dzaznieks, C. Serre, F. Millange, J. Dutour, S. Surblé & I. Margiolaki, *Science*, **2005**, *309*, 2040.19
[85] D. M. Rudkevich & A. V. Leontiev, *Aust. J. Chem.*, **2004**, *57*, 713
[86] B. Chen, C. Liang, J. Yang, D. S. Contreras, Y. L. Clancy, E. B. Lobkovsky, O. M. Yaghi & S. Dai, *Angew. Chem. Int. Ed.*, **2006**, *45*, 1390
[87] M. Albrecht, M. Lutz, A. L. Spek & G. van Koten, *Nature*, **2000**, *406*, 970
[88] T. Hertzsch, F. Budde, E. Weber & J. Hulliger, *Angew. Chem. Int. Ed.*, **2002**, *41*, 2281
[89] M. Tadokoro, S. Tasuzuka, M. Nakamura, T. Shinoda, T. Tatenuma, M. Mitsumi, Y. Ozawa, K. Toriumi, H. Yoshino, D. Shiomi, K. Sato, T. Takui, T. Mori & K. Murata, *Angew. Chem. Int. Ed.*, **2006**, *45*, 5144
[90] C. Thompson, N. R. Champness, A. N. Khlobystov, C. J. Roberts, M. Schröder, S. J. B. Tendler & M. J. Wilkinson, *J. Microscopy*, **2004**, *214*, 261

encountered and utilized gases, as summarized in Table 8. The recent interest in gas storage and separation is a direct result of "Hydrogen Economy"[91]. The effort devoted to the search for alternative fuels has increased significantly because of the awareness of the decline of fossil fuel supplies. The availability of methane and hydrogen in abundant supplies of natural gas and water has resulted in these two gases leading the race to be proclaimed the best alternative fuel.

Table 8 Common gases and their uses

Gas	Uses
Nitrogen (N_2)	80% of earth's atmosphere, nitrogen cycle in nature
Carbon dioxide (CO_2)	most recognized greenhouse gas (pollutant), photosynthesis, main product of combustion of carbon-based fuels
Methane (CH_4)	natural gas, possible replacement for fossil fuels
Oxygen (O_2)	combustion, respiration, reactant in hydrogen fuel cells
Hydrogen (H_2)	basis of the hydrogen economy, reactant in hydrogen fuel cells, believed to be the best alternative to fossil fuels

One of the most significant problems associated with using these two gases as fuels relates to the difficulties associated with their storage and transport[104]. One of the most promising approaches to solving this problems involves the reversible sorption into porous materials[92].

[91] T. Burchell & M. Rogers, SAE Technol. Pap. Ser., **2000**, 2000-01-2205
[92] A. M. Seayad & D. M. Antonelli, *Adv. Mater.*, **2004**, *16*, 765

Separation of the five gaseous compounds listed above from one another and other gases, is also an extremely important concern[83,93]. At the current level of technology, H_2 is produced commercially via the two reactions (see below).

$$CH_4 + H_2O \rightarrow CO + 3H_2$$

$$CO + H_2O \rightarrow CO_2 + H_2$$

The final product, H_2, requires substantial purification by removing impurities such as CO, CH_4, H_2O, any impurities within the natural gas and, primarily, CO_2. Both the design and implementation of separation technologies has improved to such an extent that any improvement in gas separation necessitates the development of new adsorbent materials[83].

Porosity studies of crystalline materials, are still at the beginning. Is not yet clear how surface area, shape, type of interactions at the gas/solid interface or chemical functionality of the material will improve sorption properties. Thus, this study represents an effort towards gaining insight into the nature of gas sorption phenomena[94].

A description of the gas sorption apparatus and methodology is given at the beginning of this chapter in order to disclose how the experimental results were obtained.

Applications

Research groups have already found many useful applications for the storage and release of gases from different materials such as the storage of hydrogen[95,96] and methane[97] for energy applications. Environmental

[93] S. M. Kuznicki, V. A. Bell, S. Nair, H. W. Hillhouse, R. M. Jacubinas, C. M. Braunbarth, B. H. Toby & M. Tsapatsis, *Nature*, **2001**, *412*, 720

[94] H. Chun, D. N. Dybstev, H. Kim & K. Kim, *Chem. Eur. J.*, **2005**, *11*, 3521

[95] B. Xiao, P. S. Wheatley, X. Zhao, A. J. Fleycher, S. Fox, A. G. Rossi, I.L. Megason, S. Bordiga, L. Regli, K. M. Thomas, and R.E. Morris, J. Am. Chem. Soc., 2007, 129, 1203-1209

applications of gas storage media focus on the reduction of green house gases such as the removal of carbon dioxide and sulfur dioxide from the flue exhaust of power plants. Research into medical applications is also being applied to metal organic frameworks with the storage of nitric oxide for drug delivery.

Hydrogen

Some fields of research suggest that hydrogen storage would be most viable in a metal organic framework as they have a large surface area with adsorption capacities, BASF have shown that the large surface areas of metal organic frameworks can contain a greater amount of H_2 in comparison to an empty container. Figure 50 highlights how Cu-EMOF can store twice as much hydrogen within its framework than a conventional container at 30 bar. It is often forgotten that in today's society we use gas storage every time we start our cars or fly in a plane. Hydrogen locked into the crude oil based fuel oils is done in a non-reversible way but it is done so in a highly efficient and dense medium which currently out performs any other hydrogen storage system.

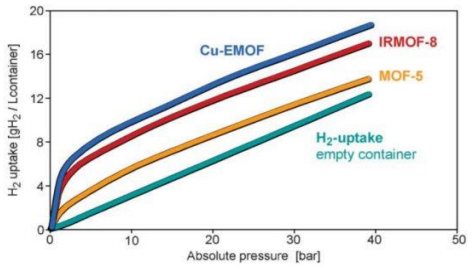

Figure 49 This graph highlights how the different MOFs (Cu-EMOF, IRMOF-8 and MOF-5) can contain more H_2 gas than a conventional gas bottle

[96] D. J. Collins and H. Zhou, J. Mater.Chem., 2007, 17, 3154-3160
[97] M. Eddaoudi, J. Kim, N. Rosi, D.Vodak, J. Watcher, M. O'Keefe, and O.M. Yaghi, Science., 2002 295, 469

Carbon Dioxide

Carbon dioxide is a greenhouse gas and a significant contributor to global warming. There is a big push at the moment by companies to minimize the amount of carbon dioxide. This can be achieved in numerous ways the most obvious being in the reduction in gas omissions from factories, transport and power production.

Chemisorption is providing one way of capturing this unwanted gas such as with activated carbon and within zeolites. However the best absorbers reported so far are from the metal organic frameworks MOF. The aim of this approach would be to capture the gas and store it underground. Other proposals have included injection of the gas into deep saline aquifers and chemical fixation.

Sulfur Dioxide

Sulfur dioxide is a toxic gas and is usually given off as a by-product in many industrial processes which can have drastic effects on the environment, it can lead to the production of acid rain. There have been some studies of sulfur dioxide adsorption and desorption in zeolites. Work by Cross et al[98] have shown that it is possible to reversibly adsorb SO_2 by MOFs. Many different conformations of SO_2 binding have been reported and as such there have been studies to investigate the most likely, such as work done by Nasluzov et al[99] or as work by Dathe et al[100] where barium was examined in an oxidative atmosphere whereby the SO_2 was adsorbed irreversibly as sulfates.

[98] W.I. Cross, S.M. Godfrey, C. A. McAuliffe and R. G. Pritchard, Chem. Commum., 2001, 1764-1765
[99] V. A. Nasluzov, A.M. Shir, F. Nörtemann, M. Staufer, I V. Yudanov, N. Rösch, Journal of Molecular Structure (theochem)., 1999, 466, 235-244
[100] H. Dathe, E. Peringer, V. Roberts, A. Jentys and J.A. Lercher, C.R. Chimie., 2005, 8, 753-763

Nitric Oxide

Nitric oxide, once known as just a toxic gas, has been found to be an extremely important biological signalling molecule for vasodilatation, the prevention of platelet aggregation and wound repair. Zeolites and MOFs have been looked at to be possible delivery systems to administer the gas in a controlled.

With these interesting applications it is desirable to understand how the gas molecules bind inside a framework, so that we may be able to improve the storage of the material or release the gases at varying rates. McKinlay et al[101] showed that it is possible to use powder X-ray diffraction to examine a nitric oxide, other has been carried out by Cruz et al[102] who were able to use single crystal data to locate nitric oxide in the cobalt exchanged zeolite-A.

[101] A.C. Mckinlay, B. Xiao, D.S. Wragg, P.S. Wheatley, I.L. Megson and R. E. Morris, J. Am. Chem. Soc., 2008, 130, 10440-10444

[102] W.V Cruz, P.C.W. Leung and K. Seff, Inorg. Chem., 1979, 18, 1692-1696

MOF

The construction of coordination polymers is of current interest for the development of new functional materials and in fundamental studies of crystal engineering and supramolecular chemistry[103,104,105,106,107,108,109,110].
In the synthesis of new network structures, coordination polymers constructed from heteroorganic bridges are challenging subjects because any synthetic method used needs to take into account the designed construction involving versatile coordination frameworks[111,112,113,114]. The unique feature of this type of network structure is the presence of square cavities, which present functionality such as gas adsorption.
In this work, we have created one new zinc coordination polymers constructed from heteroorganic bridges: Zn S N_3 O_5 C_{30} H_{29} DMF (MoF1). Fig. 51.

[103] M. Fujita, Y.J. Kwon, S. Washizu, K. Ogura, J. Am. Chem. Soc. 116 (1994) 1151
[104] J.-M. Lehn, Supramolecular Chemistry, VCH, Weinheim, 1995
[105] S.R. Batten, R. Robson, Angew. Chem., Int. Ed. 37 (1998) 1460
[106] P.J. Hagrman, D. Hagrman, J. Zubieta, Angew. Chem., Int. Ed. 38 (1999) 2638
[107] D.B. Amabilino, J.F. Stoddart, Chem. Rev. 95 (1995) 2725
[108] D.S. Lawrence, T. Jiang, M. Levett, Chem. Rev. 95 (1995) 2229
[109] M. Eddaoudi, D.B. Moler, H. Li, B. Chen, T.M. Reineke, M. O'Keeffe, O.M. Yaghi, Acc. Chem. Res. 34 (2001) 319
[110] S. Kitagawa, R. Kitaura, S. Noro, Angew. Chem., Int. Ed. 43 (2004) 2334
[111] M. Kondo, T. Okubo, A. Asami, S. Noro, T. Yoshitomi, S. Kitagawa, T. Ishii, H. Matsuzaka, K. Seki, Angew. Chem., Int. Ed. 38 (1999) 140
[112] X.-L. Wang, C. Qin, E.-B. Wang, Y.-G. Li, Z.-M. Su, L.Xu.L. Carlucci, Angew. Chem., Int. Ed. 44 (2005) 5824
[113] R. Kitaura, K. Fujimoto, S. Noro, M. Kondo, S. Kitagawa, Angew. Chem., Int. Ed. 41 (2002) 133
[114] D.N. Dybtsev, H. Chun, K. Kim, Angew. Chem., Int. Ed. 43 (2004) 5033

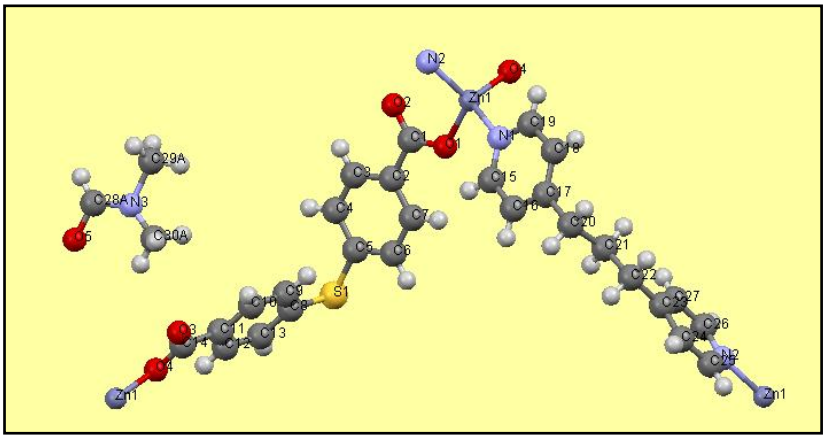

Figure 50 shows the new MOF

Results and discussion

Diffusion of a DMF/H_2O solution of Dithiobenzoic acid (DTBA) and 1,3-Di(4-pyridil)-propane (BPP) into a DMF solution of $Zn(NO_3)_2$ $4H_2O$ yielded single crystals of Compound MoF1. An ORTEP view around the zinc centers is shown in Fig. 52. The carboxylate ligands of the DTBA and the nitrogen of BPP bind to the zinc center: Zn(1)–O(1) = 1.952(2) Å, Zn(1)–O(4) = 1.934(2) Å, Zn(1)–N(1) = 2.052(3) Å and Zn(1)–N(2) = 2.004(2) Å.

Each zinc center is bridged by an DTBA group to yield a one-dimensional chain directed along the b-axis Fig. 55. The chains are further connected by BPE bridges to yield a ladder-type one-dimensional structure, as shown in Fig. 55, in which the Zn–DTBA chains construct the ‘‘side rails’’, and the Zn–BPE–Zn parts construct the ‘‘rungs’’ of the ladder framework. The Zn-Zn distances bridged by the DTBA and BPE groups are 14.55 Å and 13.20 Å, respectively, which form large cavities with an effective area of about 12-11 Å [126].

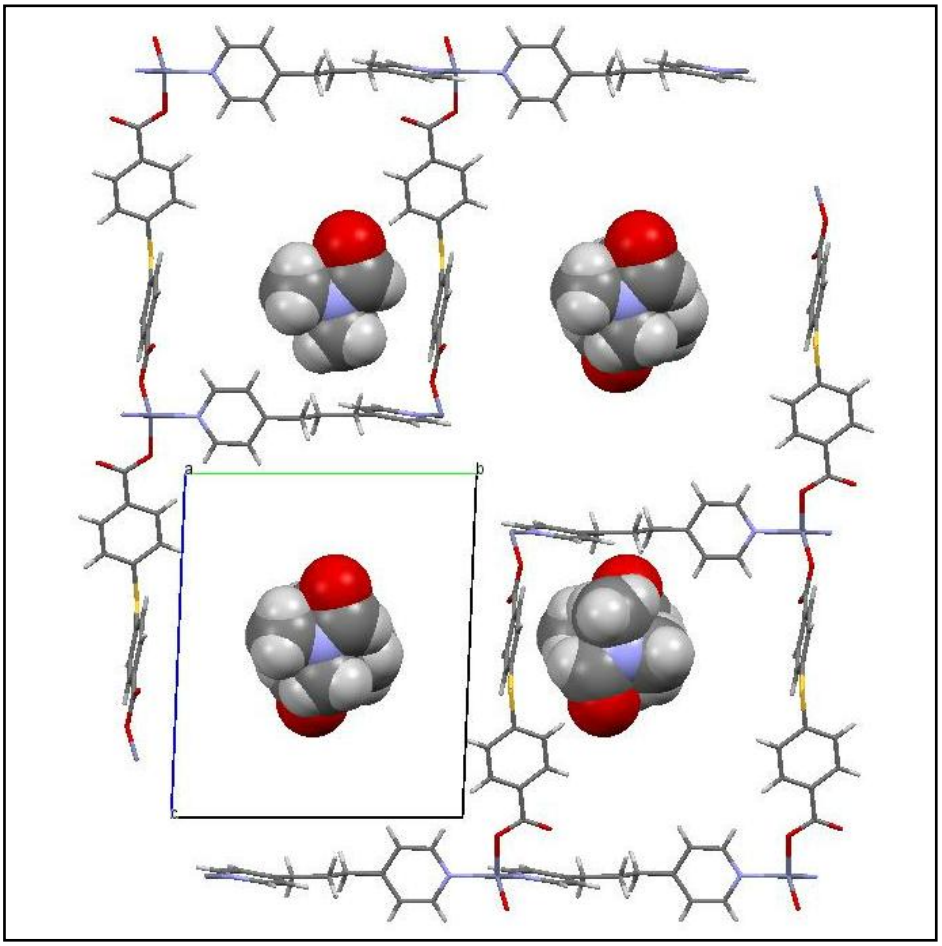

Figure 51 View along a

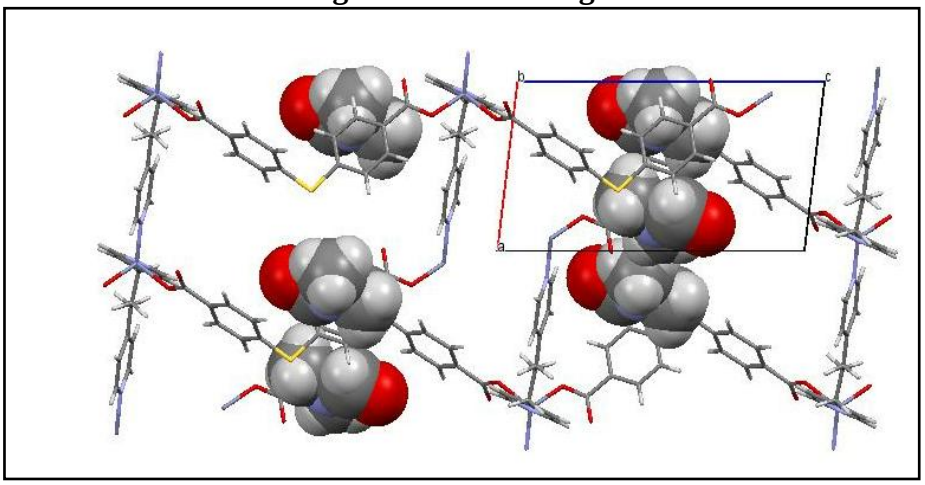

Figure 52 View along b

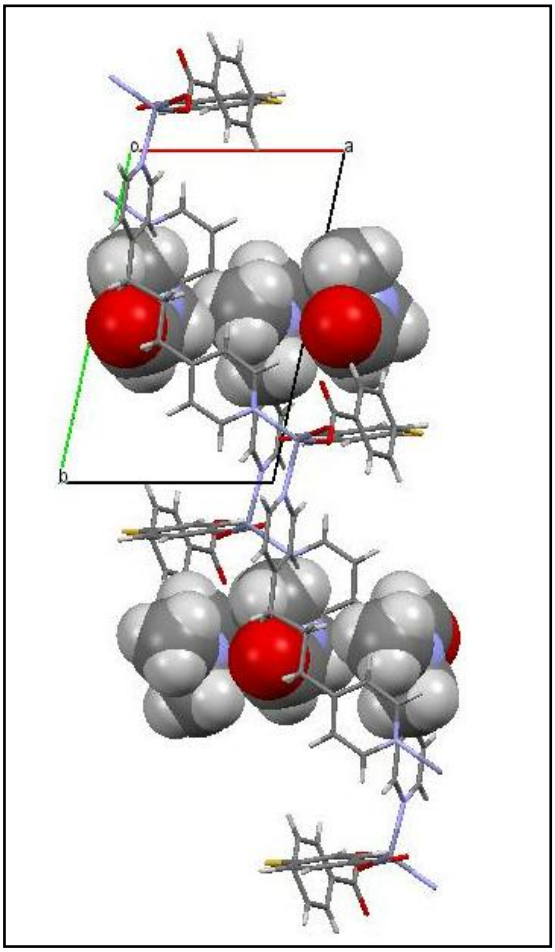

Figure 53 View along c

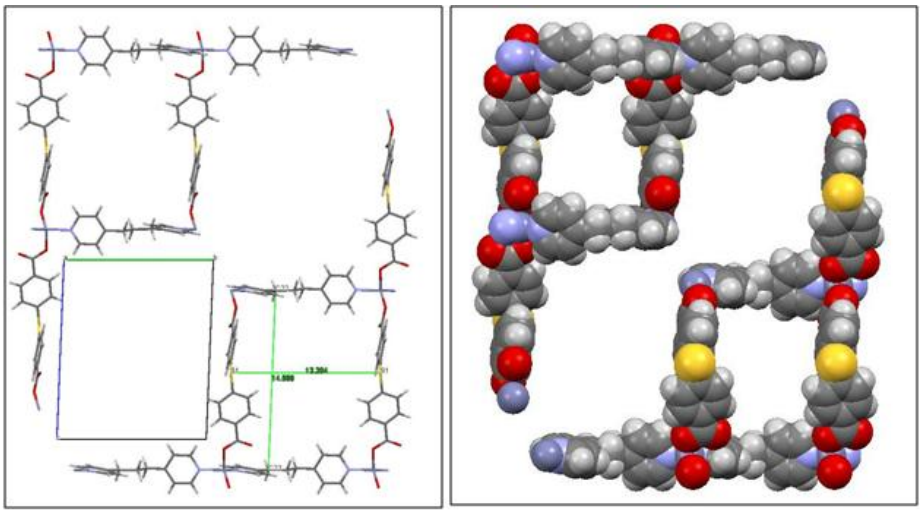

Figure 54 Cavities along a of the MOF.

The MOF presents two molecules of DMF for each cavity, the removal of the guest DMF molecules and the characterization of the functionalities based on the highly porous framework of Compound is currently in progress.

Experimental

Preparations of the compounds

The compound Zn S N_3 O_5 C_{30} H_{29} DMF was prepared by diffusion of a DMF solution (4 mL)/ H_2O (0,4 mL) of DTBA (27 mg, 0,1 mmol) and BPE (18 mg, 0,1 mmol) into a DMF solution (1 mL) of $Zn(NO_3)_2$ $4H_2O$ (37 mg, 0,1 mmol). Red columnar crystals were formed within a period of one week.

However, the acid (DTBA) was synthesized in the following way:

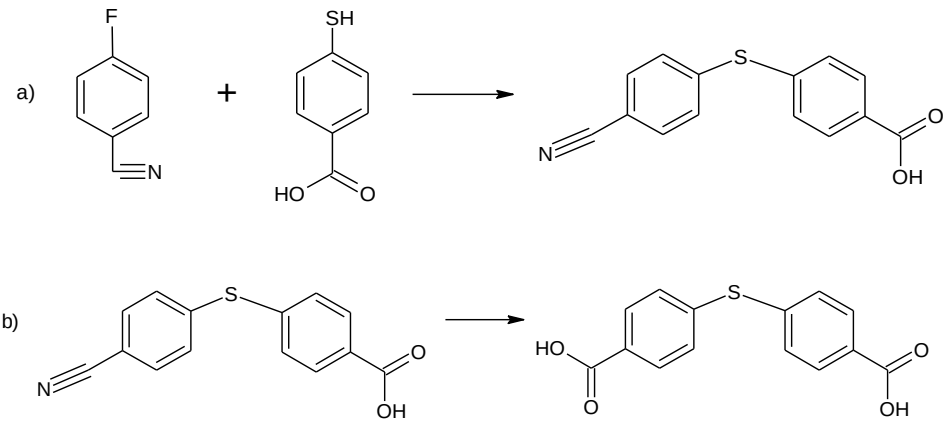

In reaction a), we synthesized the thiobenzoic p-benzonitrile acid (comp.1).

3,00 g (mol) of Mercapto benzoic acid was added to 2,1 g of p-Fluorine benzonitrile (mol) and 7,26 g (mol) K_2CO_3 in 50 mL of DMF at 100 C, the reaction was conducted at reflux for 24 h. The product was acidified with few mL of HCl (1M).

In reaction b) was obtained the DTBA by basic hydrolysis.

The (comp.1) was added to 3 g of KOH in 60 mL of etOH and 15 mL of H_2O at 100-110 C , the reaction was conducted at reflux for 24 h.

Crystal structure determination

Single crystal X-ray diffraction data were collected using the Mo Kα radiation (λ = 0.71073 E) on a SMART APEX2 diffractometer; all data were collected at low temperature (273K). The collected intensities were corrected for Lorentz and polarization factors and empirically for absorption by using the SADABS program[115]. Structures were solved by direct methods using SIR97[116] and refined by full-matrix least-squares on all F^2 using SHELXL97[117] implemented in the WinGX package[118]. Hydrogen atoms were introduced in calculated positions. Anisotropic displacement parameters were refined for all non-hydrogen atoms. Hydrogen bonds have been analyzed with SHELXL97[119] and PARST97[120] and extensive use was made of the Cambridge Crystallographic Data Centre packages[121] for the analysis of crystal packing. Table 9 summarizes crystal data and structure determination results.

[115] a) SAINT: SAX, Area Detector Integration, Siemens Analytical instruments INC., Madison, Wisconsin, USA. b) SADABS: Siemens Area Detector Absorption Correction Software, G. Sheldrick, 1996, University of Goettingen, Germany

[116] A new Program for Solving and Refining Crystal Structures, A. Altomare, M.C. Burla, M. Camalli, G. Cascarano, C. Giacovazzo, A. Guagliardi, A.G. Moliterni, G. Polidori, R. Spagna, 1997, Istituto di Ricerca per lo Sviluppo di Metodologie Cristallografiche CNR, Bari

[117] [117] Shelxl97. Program for structure refinement, G. Sheldrick, University of Goettingen, Germany, 1997

[118] L.J. Farrugia, J. Appl. Cryst., 1999, 32, 837–838

[119] M. Nardelli, J. Appl. Cryst., 1995, 28, 659

[120] M. Nardelli, J. Appl. Cryst., 1995, 28, 659

[121] a) F.H. Allen, O. Kennard, R. Taylor, Acc. Chem. Res., 1983, 16, 146–153; b) I.J. Bruno, J.C. Cole, P.R. Edgington, M. Kessler, C.F. Macrae, P. McCabe, J. Pearson, R. Taylor, ActaCrystallogr. 2002, B58, 389–397

Table 9 Crystal data and structure refinement

	MOF	
Empirical formula	$C_{30}H_{29}N_3O_5SZn$	
Formula weight	608,99	
Temperature	293(2) K	
Wavelength	0.71073 Å	
Crystal system, space group	triclinic, P-1	
Unit cell dimensions	a = 7.978(2) Å	α = 90.783(4)°
	b = 12.351(3) Å	β = 96.757(4)°
	c = 14.589(4) Å	γ = 102.259(3)°
Volume	1393.8(6) $Å^3$	
Z, Calculated density	2, 1.451Mg/m^3	
Absorption coefficient	0.875 mm^{-1}	
F(000)	632	
Crystal size	0.140	
Theta range for data collection	1.689° to 25.974°	
Limiting indices	$-9\leq h\leq 9$, $-12\leq k\leq 15$, $-17\leq l\leq 15$	
Completeness to theta	5310 / 394 [R(int) = 0.0417]	
Refinement method	95.5 %	
Data / restraints / parameters	Full-matrix least-squares on F^2	
Goodness-of-fit on F^2	1830 / 0 / 198	
Final R indices [I>2sigma(I)]	1.063	
R indices (all data)	R_1 = 0.0417, wR_2 = 0.1209 R_1 = 0.0535, wR_2 = 0.1341	
Largest diff. peak and hole	0.323 and -0.233 $e\cdot Å^{-3}$	

Conclusion

We have obtained a new MoF, it is composed of Zn coordinated with four organic ligands: two molecules of DTBA and two molecules of BPE. The MoF presents very large square cavity. In the future it will be studied the capacity of adsorbtions in liquid phase and gas phase of this system.

Part III: Study on the crystal packing of two amino-hydroxybenzoic acids

Introduction

A complete understanding of the rules governing the self-assembly in the solid state is an attractive goal to pursue, as this would be the key requisite for designing new materials with the desired physico-chemical properties. Unfortunately most of the factors playing an important role in determining the final crystal packing are hardly quantifiable; nowadays it is not possible to know *a priori* how a given molecule will exactly crystallize[122], even if a significant progress in crystal structure prediction has been achieved in the last years, thanks to the use of computational methods increasingly powerful for calculating the energetically most probable form[123]. However, since the crystallization process is an event under kinetic control, it often happens that the final observed structure is not the thermodynamically favored form, but simply the easiest and/or fastest to obtain. In this context, it is of fundamental importance the role of the Cambridge Structure Database (CSD) as a huge resource of information included in hundreds of thousands of deposited structures, from which it is possible to obtain statistics on the supramolecular motifs and derive a hierarchy between them, on the basis of their robustness[124]. In the present chapter we analyze the solid state behaviour of two organic molecules,

[122] A. Gavezzotti, Acc. Chem. Res., 1994, 27, 309–314
[123] a) S.M. Woodley, R. Catlow, Nature Materials, 2008, 7, 937–946; b) C.W. Lehmann, Angew. Chem. Int. Ed. 2011, 50, 5616–5617
[124] A. Bacchi, Engineering of Crystalline Materials Properties, NATO Science for Peace and Security Series B: Physics and Biophysics, 2008, 33–58

4-amino-3-hydroxybenzoic acid (**1**) and 3-amino-4-hydroxybenzoic acid (**2**) (Fig. 56): these two compounds have been extensively used by our research group as ligands for the synthesis of several wheel-and-axle metallorganic (WAAMO) complexes[125]. In particular in our systems they constituted the linear central spacer, that was built by exploiting the hydrogen bond interaction between two carboxylic functions, generating a sort of supramolecular dimer (Figure 57).

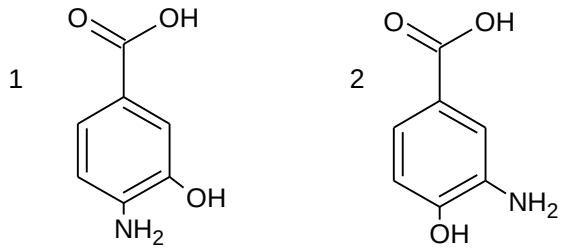

Figure 55 4-amino-3-hydroxybenzoic acid (1) and 3-amino-4-hydroxybenzoic acid (2)

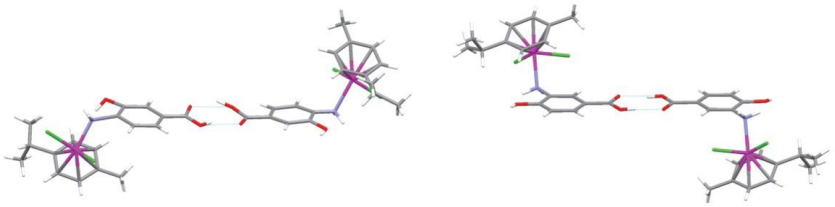

Figure 56 Examples of Ru-WAAMO: [(p-cymene)Ru(4-amino-3-hydroxybenzoic acid)Cl_2] (left) and [(p-cymene)Ru(3-amino-4-hydroxybenzoic acid)Cl_2] (right)

Although these two molecules are very similar, since they only differ in the position of the amino and hydroxy groups, their crystal packing shows some interesting differences that we have tried to rationalize on the basis of the acid-base behavior of the two molecules, and by comparing them with other similar structures present in the CSD. In particular we are interested in the occurring of the supramolecular dimerization between the

[125] A. Bacchi, G. Cantoni, F. Mezzadri, P. Pelagatti, Cryst. Growth Des., 2012, 12, 4240–4247

functions of the carboxylic acid, generating $R^2(8)$ synthon in the graph set notation[126]. This supramolecular ring occurs for 95% of nonfunctionalized monocarboxylic acid[127] when no other hydrogen bond accepting competitors are present, and reduces to 33% in general cases[128].

Results and Discussion

4-amino-3-hydroxybenzoic acid (**1**) and 3-amino-4-hydroxybenzoic acid (**2**) are commercially available and were used as received. Single crystals suitable for X-ray diffraction experiments were obtained by slow evaporation at room temperature of a saturated solution of **1** and **2** in methanol and dichloromethane, respectively, but in the case of **2** an inert atmosphere of dry nitrogen was necessary for obtaining the anhydrous form. In fact all the crystallization experiments of compound **2** carried out in different solvents without the use of the glove box equipment lead always to the same monohydrated crystal form, already present in the Cambridge Structure Database.

Molecular structure and labeling of **1** and **2** are shown in Figure 58. The two molecules are substantially planar except for a small deviation from the plane of the –COOH group (C3–C2–C1–O1 = 10.92° for **1** and C2–C1–C7–O1 = 7.68° for **2**).

[126] a) M.C. Etter, Acc. Chem. Res., 1990, 23, 120; b) J. Berstein, R.E. Davis, L. Shimoni, N.- L. Chang, Angew. Chem. Int. Ed., 1995, 34, 1555
[127] T. Beyer, S.L. Price, J. Phys. Chem. B, 2000, 104, 2647
[128] F.H. Allen, W.D.S. Motherwell, P.R. Raithby, G.P. Shields, R. Taylor, New J. Chem., 1999, 23, 25

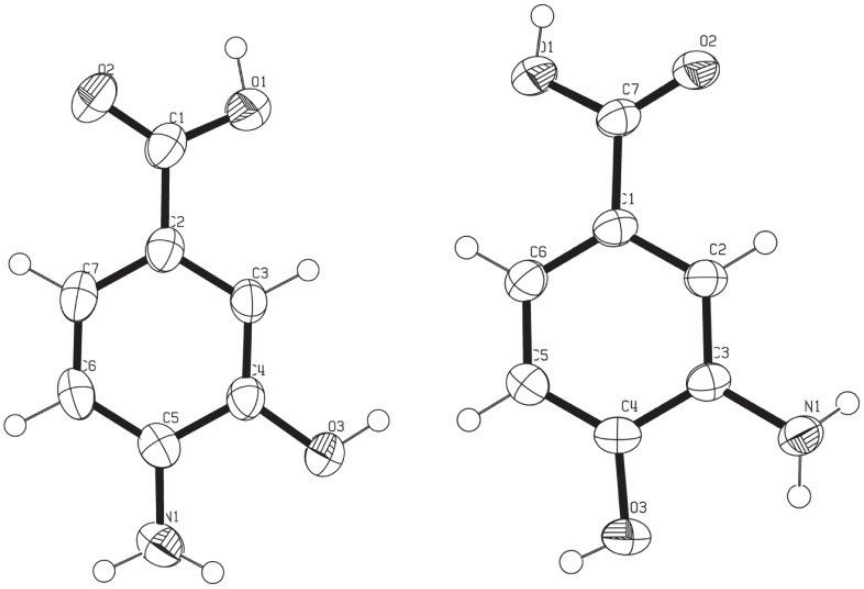

Figure 57 Molecular structure and labeling of 1 (left) and 2 (right)

The solid state packing of **1**, crystallized in an orthorhombic Pcab space group, is determined by the presence of two hydrogen bonds involving the -COOH, -OH and -NH_2 groups: -O1-H···N1 [O1···N1 (x, 1/2+y, 1/2-z) = 2.764(2) Å, 166.28(2)°], –O3–H···O2 [O2···O3 (1/2+x, -y, 1/2-z) = 2.683(1) Å, 165.74(2)°] (Figure 59); these two interactions generate antiparallel chains along *a* and zig-zag chains along *b* (Figure 60 left); the layers are then stacked through the contact N1–H···O2 [N1···O2 (1/2-x, 1/2+y, 1-z) = 3.12(1) Å, 141.4(2)°] and through π-π contacts between the phenyl units (Figure 60 right).

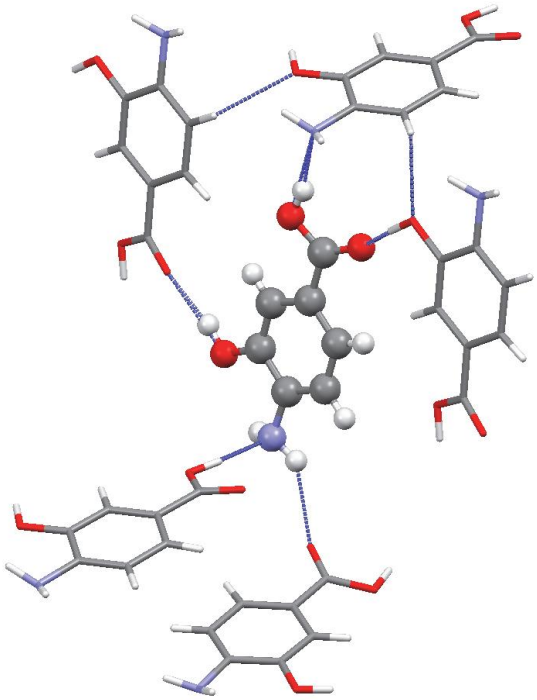

Figure 58 Hydrogen bonds of 1

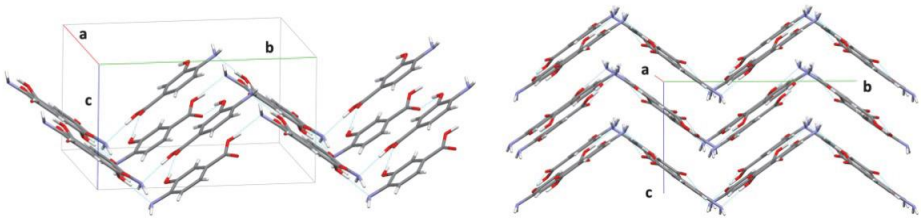

Figure 59 Chains formed by 1 (left) and their stacking (right)

An interesting analogy with this packing can be found in one of the crystal forms of 4-aminobenzoic acid present on the CSD, in particular in the structure named **AMBNAC04**[129]. In this case we find again an interaction –OH···N which leads to the formation of zig-zag chains, very similar to what discussed in **1** (Figure 61); due to the absence of the hydroxyl group,

[129] S.Gracin, A.Fischer, Acta Crystallogr., Sect.E: Struct.Rep.Online, 2005, 61, o1242

here the C=O group contacts a close –NH2 group through an hydrogen bond, with the resulting formation of a supramolecular ring synthon, which is closed by the presence of another carboxylic group. This finite motif is accompanied by the construction of supramolecular rectangles of two different sizes.

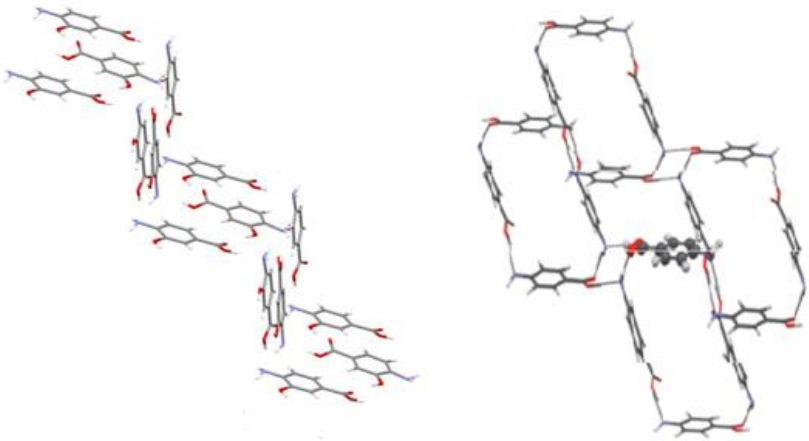

Figure 60 Comparison between the packing of 1 (left) and AMBNAC04 (right)

3-amino-4-hydroxybenzoic acid (**2**) crystallizes in a monoclinic P21/c space group; here we observe the formation of a supramolecular dimer, generated by the hydrogen bonds between the carboxylic functions of two different molecules: O1–H···O2 [O1···O2 (-2-x, 2-y, 1-z) = 2.650(1) Å, 173.20(7)°] (Figure 62). A hydrogen bond, typical of 2-aminophenols[130], occurs between the alcoholic function and the amino group, O3–H···N1 [O3···N1 (-x, -1/2+y, 1/2-z) = 2.746(1) Å, 156.20(7)°]; this motif generates an helical polymer (Figure 65) along b, and polymers of alternating helicity, connected in zig-zag chains by the formation of the supramolecular dimer (Figure 63), may be considered to lay in sheets; inter-helix interactions seem to be mediated by stacking of the

[130] M. Haisa, S. Kashino, T. Kawashima, ActaCrystallogr., Sect. B: Struct. Crystallogr. Cryst. Chem., 1980, 36, 1598–1601

(carbonyl)phenyl groups and by an interaction N–H···O=C, linking homochiral helices: N1–H···O2 [N1···O2 (-1-x, -1/2+y, 1/2-z) = 3.13(1) Å, 170.6(3)°].

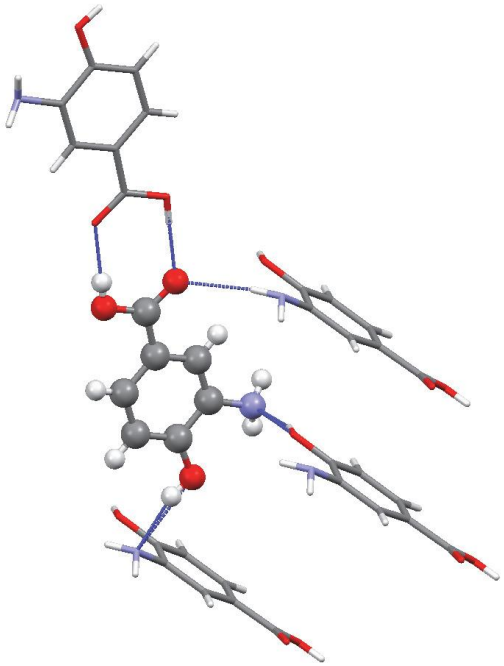

Figure 61 Hydrogen bonds of 2

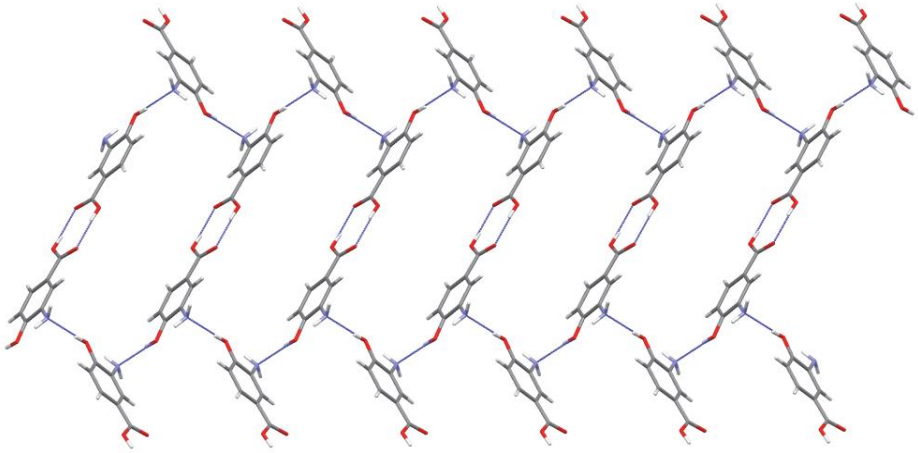

Figure 62 Polymers of alternating helicity connected by the formation of the supramolecular dimer in 2

At this point we were interested to know how the packing would change in absence of the hydroxyl group: for this reason we studied the four structures of 3-aminobenzoic acid reported on a work by D.M. Harris *et al.*[131] and on the CSD. In two of them (Form **III** and **IV**) our molecule exists as a zwitterionic tautomer, while in Form **II** and **V** the supramolecular dimerization between the COOH functions is observed. The packing of Form **II** (**AMBNZA**) and **V** [10] are dominated by a series of NH···N and NH···O interactions (Figure 64); two different types of chains are generated.

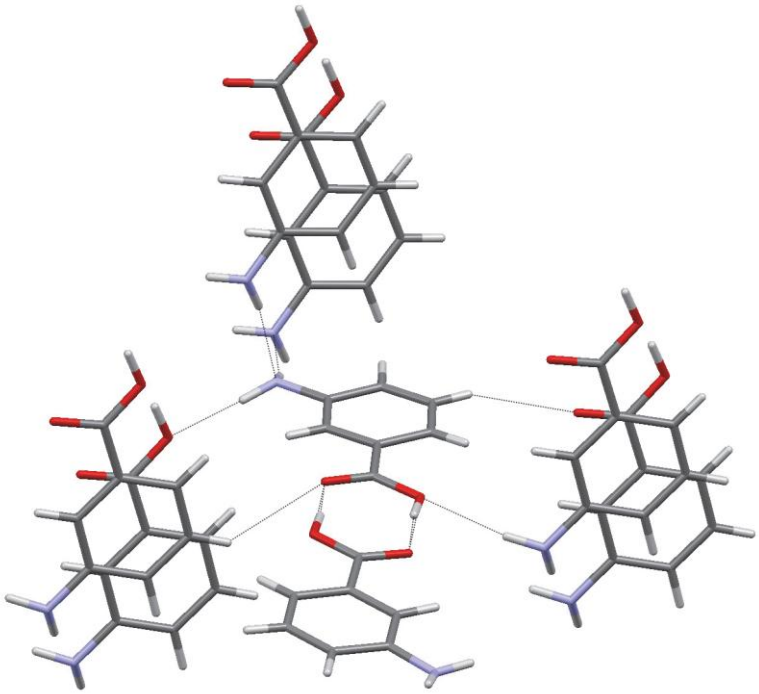

Figure 63 Interactions of AMBNZA

[131] P.A. Williams, C.E. Hughes, G.K. Lim, B.M. Kariuki, K.D.M. Harris, Cryst. Growth Des., 2012, 12, 3104 3113

A possible explanation of the crystallization of this zwitterionic form is that the presence of water may promote the precipitation of this form instead of that non zwitterionic. This hypothesis is confirmed by the solid state packing, where we can observe that the water establishes four hydrogen bonds with two –COOH and one NH2 groups of four different molecules: –Ow–H···O1 [Ow···O1 (1-x, -1/2+y, 1/2-z) = 2.903(2) Å, 168.75(2)°], –Ow–H···O2 [Ow···O1 (-1/2+x, y, 1/2+z) = 2.694(1) Å, 171.1(2)°], –O3–H···Ow [O3···Ow (-1/2+x, y, 1/2-z) = 2.646(3) Å, 166.03(1)°], –N1–H···O4 [N1···O4 (x, 1/2-y, -1/2+z) = 2.896(2) Å, 157.37(3)°].

We think that an important role in generating this solvated structure is played by the -OH group: in fact, being the -OH an electron attractor group, it will make the hydrogen on the carboxylic group in para position more acid and therefore easier to pull off by the aminic nitrogen.

Experimental

4-amino-3-hydroxybenzoic acid (**1**) and 3-amino-4-hydroxybenzoic acid (**2**) are commercially available and were used as received. Single crystal X-ray diffraction data were collected using the Cu Kα radiation (λ = 1.54178 Å) on a Siemens diffractometer for **1** and the Mo Kα radiation (λ = 0.71073 Å) on a SMART APEX2 diffractometer for **2**; all data were collected at room temperature (293K). The collected intensities were corrected for Lorentz and polarization factors and empirically for absorption by using the SADABS program[132]. Structures were solved by direct methods using SIR97[133] and refined by full-matrix least-squares on all F2 using SHELXL97[134] implemented in the WinGX package[135]. Hydrogen atoms were introduced in calculated positions; the different lengths of the C=O and C–OH bonds confirm the presence or absence of the zwitterionic tautomerization. Anisotropic displacement parameters were refined for all non-hydrogen atoms. Hydrogen bonds have been analyzed with SHELXL97[156] and PARST97[136] and extensive use was made of the Cambridge Crystallographic Data Centre packages[137] for the analysis of crystal packing. Table 10 summarizes crystal data and structure determination results.

[132] a) SAINT: SAX, Area Detector Integration, Siemens Analytical instruments INC., Madison, Wisconsin, USA. b) SADABS: Siemens Area Detector Absorption Correction Software, G. Sheldrick, 1996, University of Goettingen, Germany
[133] Sir97: A new Program for Solving and Refining Crystal Structures, A. Altomare, M.C. Burla, M. Camalli, G. Cascarano, C. Giacovazzo, A. Guagliardi, A.G. Moliterni, G. Polidori, R. Spagna, 1997, Istituto di Ricerca per lo Sviluppo di Metodologie Cristallografiche CNR, Bari
[134] Shelxl97. Program for structure refinement, G. Sheldrick, University of Goettingen, Germany, 1997
[135] L.J. Farrugia, J. Appl. Cryst., 1999, 32, 837–838
[136] M. Nardelli, J. Appl. Cryst., 1995, 28, 659
[137] a) F.H. Allen, O. Kennard, R. Taylor, Acc. Chem. Res., 1983, 16, 146–153; b) I.J. Bruno, J.C. Cole, P.R. Edgington, M. Kessler, C.F. Macrae, P. McCabe, J. Pearson, R. Taylor, ActaCrystallogr. 2002, B58, 389–397

Table 10

	1		2	
Empirical formula	$C_7H_7NO_3$		$C_7H_7NO_3$	
Formula weight	153.14		153.14	
Temperature	293(2) K		293(2) K	
Wavelength	1.54178 Å		0.71073 Å	
Crystal system, space group	orthorhombic, Pcab		monoclinic, $P2_1/c$	
Unit cell dimensions	a = 11.7556(6) Å	α = 90°	a = 5.2393(13) Å	α = 90°
	b = 14.2695(14) Å	β = 90°	b = 7.6960(19) Å	β = 92.593°
	c = 8.1898(4) Å	γ = 90°	c = 16.942(4) Å	γ = 90°
Volume	1373.81(17) $Å^3$		682.4(3) $Å^3$	
Z, Calculated density	8, 1.481 Mg/m^3		4, 1.490 Mg/m^3	
Absorption coefficient	0.118 mm^{-1}		0.118 mm^{-1}	
F(000)	640		320	
Crystal size	0.1 x 0.08 x 0.06 mm		0.1 x 0.07 x 0.05 mm	
Theta range for data collection	2.85° to 25.64°		2.41° to 27.45°	
Limiting indices	$-2\leq h\leq 14$, $-16\leq k\leq 17$, $-9\leq l\leq 9$		$-6\leq h\leq 6$, $-9\leq k\leq 9$, $-21\leq l\leq 21$	
Reflections collected / unique	2415 / 1279 [R(int) = 0.0258]		8598 / 1552 [R(int) = 0.0250]	
Completeness to theta	98.8%		99.9%	
Refinement method	Full-matrix least-squares on F^2		Full-matrix least-squares on F^2	
Data / restraints / parameters	1279 / 0 / 129		1552 / 0 / 109	
Goodness-of-fit on F^2	0.785		0.709	
Final R indices [I>2sigma(I)]	R_1 = 0.0363, wR_2 = 0.1081		R_1 = 0.0340, wR_2 = 0.1184	

R indices (all data)	R_1 = 0.0387, wR_2 = 0.1127	R_1 = 0.0390, wR_2 = 0.1294
Largest diff. peak and hole	0.183 and -0.233 e·Å^{-3}	0.277 and -0.163 e·Å^{-3}

Crystallization experiments

4-amino-3-hydroxybenzoic acid (**1**) and 3-amino-4-hydroxybenzoic acid (**2**) were purchased from Sigma-Aldrich and used as received. Crystals of 4-amino-3-hydroxybenzoic acid were obtained by slow evaporation of a saturated solution of **1** in different solvents, such as dichloromethane, *n*-hexane, cyclohexanone, *n*-pentane, chloroform, ethanol, methanol etc. The experimental procedure was the following: about 30 mg of 4-amino-3-hydroxybenzoic acid were dissolved in ca. 4 mL of the respective solvents, filtered, and kept for slow evaporation at room temperature. Single crystals suitable for X-ray diffraction were obtained over a period of two days to a fortnight. 3-amino-4-hydroxybenzoic acid was crystallized from a saturated solution in dry dichloromethane: about 30 mg of **2** were dissolved in ca. 4 mL of the dry solvent, filtered, and kept for slow evaporation at room temperature in glove box in inert atmosphere of dry nitrogen; single crystals were obtained after a week.

Conclusion

In this chapter we have studied the crystal packing of two amino hydroxybenzoic acids, underlining the common features and trying to give an explanation to their different solid state behaviour; furthermore a comparison with other similar structures reported on the CSD has been performed, demonstrating that the Cambridge Structural Database is a powerful source of information and a tool of fundamental importance in the field of crystal engineering.

APPENDIX: Identification of TPB Polymorphs *via* Raman Spectroscopy

Raman investigation of polymorphism in 1,1,4,4-tetraphenyl-butadiene

Alessia Bacchi, Ivano Bilotti, Aldo Brillante, Domenico Crocco, Raffaele G. Della Valle, Alberto Girlando, Matteo Masino, Paolo Pelagatti and Elisabetta Venuti. *Journal of Raman Spectroscophy*. 44 (2013) 905-908. DOI 10.1002/jrs.4278

In this work, we have studied the organic molecular materials by Raman Spectroscopy because they are attracting growing attention for their applications in micro- and opto-electronics. It is rather obvious that the understanding of the connection between molecular structure, crystal packing and lattice phonon dynamics on one hand and charge transport and optical properties on the other is essential for the improvement of device structure and performance. In the last few years, we have developed and refined a methodology based on low-wavenumber (10–150 cm^{-1}) Raman spectroscopy coupled to lattice dynamics calculations to characterize crystal packing and phonons in functional molecular materials[138,139]. In this chapter, we report the Raman investigation of polymorphism of a well-known blue-emitting molecule, 1,1,4,4-tetraphenyl-butadiene (TPB), which retains its luminescent properties in the crystalline state. Actually, the solid state properties of this molecule have been poorly investigated, at least until it has been shown that one

[138] A. Brillante, I. Bilotti, R.G. Della Valle, E. Venuti, M. Masino, A. Girlando, Adv. Mat. 2005, 17, 2549
[139] A. Brillante, I. Bilotti, R.G. Della Valle, E. Venuti, A. Girlando. CrystEng- Comm 2008; 10, 937

particular polymorph exhibits amplified spontaneous emission, and could therefore be used for building a laser[140]. The TPB case is particularly intriguing, since so far we have identified four polymorphs[141,142], which differ not only in the crystal packing, but also in the molecular conformation, with different orientation of the pendant phenyl groups.

Crystal growth

TPB was purchased from Sigma Aldrich and used as received. The precise methodology for obtaining four different crystalline polymorphs is described elsewhere[52,53]. Here, we give only a short summary. α-TPB is the most commonly encountered polymorph and can by prepared by sublimation, melting followed by slow cooling, or crystallization from a variety of solvents. β-TPB can only be obtained by physical vapor transport method[52]. γ-TPB is non reproducibly obtained by crystallization from ethyl- or butyl-acetate. δ-TPB is obtained by melting at 200°–202°C followed by relatively fast cooling.

Raman measurements

The Raman spectra are a courtesy by Ondax Inc. The spectra have been obtained by a Renishaw InVia microspectrometer, with 514.4 nm excitation from an Ar laser (spectral resolution 8 cm^{-1}, laser power 2-3 mW at the sample). In order to obtain the Raman spectra close to the

[140] S. Tavazzi, L. Silvestri, L. Miozzo, A Papagni, P. Spearman, S. Ianelli,A. Girlando, A. Camposeo, M. Polo, D. Pisignano, ChemPhysChem 2010; 11, 429
[141] A. Girlando, S. Ianelli, I. Bilotti, A. Brillante, R. G. Della Valle, E. Venuti, M. Campione, S. Mora, L. Silvestri, P. Spearman, S. Tavazzi. Crystal Growth & Design 2010; 10, 2752
[142] A. Girlando et al., to be published

exciting line, three Ondax filters have been used in conjunction with the Renishaw single monochromator.

One was a narrow-band 90/10 beamsplitter, reflecting only the exciting line and Rayleigh scattering, in order to transmit most of the Raman signal and to provide O.D. 1 rejection of the Rayleigh scattering itself. Behind the beamsplitter, two narrowband Ondax notch filters have been introduced, each with O.D. of 4.0 for the Rayleigh line. All the filters block signals within about 5 cm^{-1} from the excitation wavelength, giving stray light rejection similar to that obtainable by a triple monochromator[52].

Computational methods

The adopted computational approach is fully described elsewhere[143], so that only a brief summary will be given here. We initially deal separately with intra- and inter-molecular (or lattice) vibrations, within the so-called rigid molecule approximation. The equilibrium molecular geometry and vibrations are calculated by standard DFT methods, whereas for the crystalline structure we start from the experimental X-ray data and locate the minimum of an empirical potential, represented by an atom–atom Buckingham model plus a Coulomb term. The second derivative of this potential yields the dynamical matrix, hence the lattice phonon frequencies and eigenvectors. The coupling between lattice phonons and low-wavenumber intra-molecular vibrations is then introduced by a perturbative approach[144].

[143] A. Girlando, L. Grisanti, M. Masino, I. Bilotti, A. Brillante, R. G. Della Valle, E. Venuti. Phys.Rev. B 2010; 82, 035208

[144] E. Venuti, R. G. Della Valle, L. Farina, A. Brillante, M. Masino, A. Girlando. Phys. Rev. B 2004; 70, 104106

Low frequency Raman Spectra

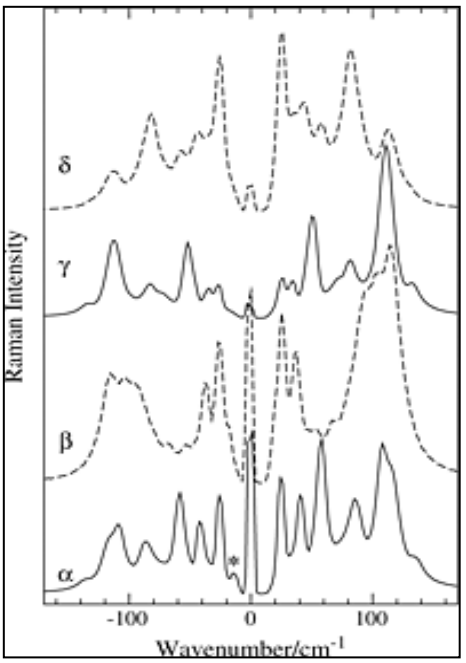

Figure 64

The low-wavenumber Raman spectra characterize the lattice (inter-molecular) phonons, which are the most sensitive to the crystalline packing. This fact can be seen immediately at the level of selection rules, which we report here in the rigid molecule approximation for the four identified polymorphs of TPB.

α-TPB crystallizes in the monoclinic system, space group $P2_1$ (C_2^2), with two molecules in unit cell, located at general positions[52,145]. Therefore, we expect nine Raman active lattice phonons, five of A symmetry, with crystal polarizability components aa, bb, cc, ac and four of B symmetry, with ab, bc components.

[145] K. Baba, H. Kasai, S. Okada, H. Oikawa, H. Nakanishi. Opt. Mater. 2002; 21, 591

β-TPB is monoclinic centrosymmetric, $P2_1/c$ (C_{2h}^5), with four molecules in the unit cell, all in general positions[52]. We have 12 Raman active phonons, six (aa,bb,cc,ac) and six Bg (ab,bc).

γ-TPB is triclinic centrosymmetric, space group P-1; (C_i^1) Z = 2^9.

We expect six Raman active phonons, all belonging to the totally symmetric, Ag, representation.δ-TPB, like γ-TPB, is triclinic centrosymmetric P-1 (C_i^1), but with three molecules in the unit cell, one located at the inversion center, and the other two in general positions[53]. We have nine Ag Raman active phonons.

The low-wavenumber Raman spectra of the four polymorphs are reported in Fig. 65. The collection of both the Stokes and anti-Stokes lines allows for a rough estimation of the sample temperature under the laser irradiation, and it shows that indeed the sample has not been heated with the used laser power. Notice the strong attenuation of the Rayleigh line. The spectra in Fig. 65 have been collected on the most developed crystal face, without taking into account the polarization of incident and scattered light with respect to the crystal orientation. In these conditions, the collected data still allow us to discriminate the different polymorphs, but do not offer an exhaustive characterization of their lattice dynamics. Moreover, in a flexible molecule like TPB, there are several low-wavenumber intra-molecular modes which strongly mix with the lattice phonons. For instance, in all the spectra, one can see a band or a group of bands around 110 cm^{-1}, whereas in the rigid molecule approximation, the highest calculated lattice frequencies are around 100 cm^{-1}. The band(s) around 110 cm^{-1} likely have intra-molecular origin, and the rigid molecule approximation is not strictly valid. For these reasons, the assignment of low-wavenumber Raman spectra of the four TPB polymorphs is a complex task, still under progress in our laboratory. Nevertheless, the rigid

molecule approximation constitutes a first useful step towards this goal. Such preliminary assignment, based on Fig. 65 and the lattice dynamics calculations performed within the rigid molecule approximation, are reported in Table 11.

Table 11 Preliminary assignment of the low-wavenumber Raman bands of the four TPB polymorphs (Fig.45). Frequencies in cm−1. The reported frequencies, calculated in the rigid molecule approximation, correspond to the structure at the minimum potential energy

α			β			γ		δ	
Exp	Cal	Sym	Exp	Cal	Sym	Exp	Cal	Exp	Cal
	18,0	A		32,1	Ag	26	28,9	25	31,8
24	32,4	A	24	32,7	Bg	35	39,1	43	45,1
41	45,4	A	37	38,9	Ag	52	62,4		48,4
58	48,2	B		40,1	Bg		65,9	58	54,2
	51,0	B		42,8	Ag	71	70,8		60,1
	53,1	A	54	55,6	Bg	82	89,6		65,8
86	83,3	B	67	57,6	Ag				75,2
	103,0	A		65,5	Bg			82	86,4
	104,9	A		74,8	Bg				100,4
			78	78,4	Ag				
				86,2	Ag				
			94	93,1	Bg				

Table 12 Lattice parameters of TPB. The room temperature experimental structures of α, β, γ and δ-TPB are compared to the calculated structures at the minimum of the potential energy Φ. Unit cell axes a, b, c are in Å, angles α, β and γ in degrees. Energies Φ in kcal/mol

	α	β	γ	δ
a_{exp}	6,259	9,736	9,820	9,835
a_{calc}	6,353	9,641	9,722	9,769
b_{exp}	22,164	8,634	10,110	10,222
b_{calc}	22,136	9,043	9,894	10,153
c_{exp}	7,362	24,480	10,851	16,060
c_{calc}	7,171	24,579	11,804	16,058
α_{exp}	90	90	99,31	83,79
α_{calc}	90	90	98,55	83,15
β_{exp}	96,35	97,11	103,64	76,41
β_{calc}	94,24	98,78	108,92	76,62
γ_{exp}	90	90	94,95	87,92
γ_{calc}	90	90	93,03	87,37
Φ_{calc}	-35,44	-32,73	-33,17	-35,01

High-wavenumber Raman spectra

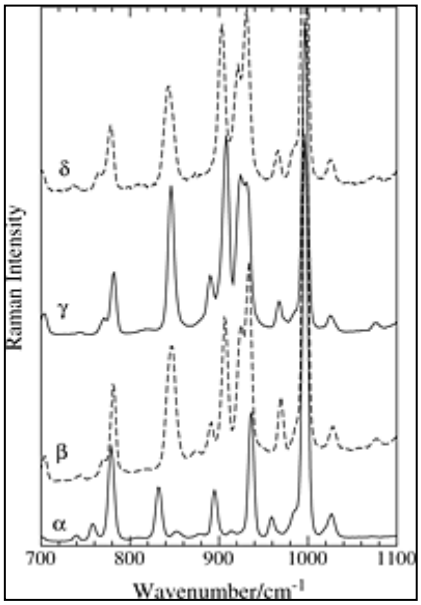

Figure 65

As already noted[52], TPB assumes a different molecular conformation, with approximate C_i and C_2 symmetries in the α and β polymorphs, respectively. As a consequence, spectral differences between the polymorphs are not limited to the region of lattice phonons, but can be found (though at lesser extent) also in the region of intra-molecular vibrations. In the γ polymorph, the TPB conformation is similar to that of the β polymorph, so we expect the high-wavenumber Raman spectra of the β and γ polymorphs to be rather similar, and clearly different from those of α-TPB. The δ-TPB unit cell, on the other hand, has one molecule with C_i symmetry, and two with approximate C_2 symmetry. In this case, we should have a sort of combination between the spectra of α- and β-TPB. By carefully looking at the Raman spectra, we have identified the CH bending/CC stretching-bending spectral region (700 cm^{-1}) as the most discriminating between the four phases, as shown in Fig.66. A detailed

assignment and interpretation of the spectra to understand in detail the origin of such differences is beyond the aim of the present paper. However, it is clear from the figure that the origin of the spectral differences is the above mentioned difference in the molecular conformation. For instance, focus the attention to the bands around 890-940 cm^{-1}, corresponding to CH bending modes. The band pattern of the β and γ polymorphs, where TPB has approximate C_2 symmetry, is quite similar and clearly different from that of a polymorph. On the other hand, δ-TPB band pattern is a sort of superposition of those of the other polymorphs. Therefore, highwavenumber Raman spectra are useful to identify the TPB polymorphs and constitute a consistency check with respect to the low-wavenumber spectral data.

Discussion and Conclusions

The Raman spectra have been instrumental in the progressive discovery of new polymorphs of TPB. In particular, the difference in the Raman spectra in microcrystalline domains has allowed the identification of two new polymorphs, β-TPB[51] and δ-TPB[53]. These were initially seen in different spots of microcrystalline samples or in different crystals inside a given batch. Being a nondestructive technique, we could then use Raman measurements to pick up the crystals more suitable for X-ray analysis, and quickly verify the results of the different preparation methods for obtaining the four polymorphs. The X-ray coordinates have been the starting point for the lattice dynamics calculations, which assist a preliminary band assignment and give an estimate of the lattice potential energy (Φ). This latter datum is reported in Table 2, where we also compare the computed unit cell parameters with the experimental ones. The agreement with the experiments gives us confidence about the overall results of calculations. The α-polymorph has the lowest potential energy minimum, therefore it appears to be the thermodynamically stable phase. Indeed, this is by far the most frequently encountered polymorph. The β and γ polymorphs have higher energies, and both appear to be difficult to prepare. On the other hand, δ-TPB is the second stable polymorph and might become the thermodynamically stable phase at temperatures close to the melting point.

Acknowledgements

I would like to thank my supervisors Prof. Alessia Bacchi and Prof. Alberto Girlando for their scientific support and collaboration to this PhD thesis, for their helpfulness, and for giving me the opportunity to attend international conferences and schools.

I wish to thank all the members of the research group: Prof. Mauro Carcelli, Prof. Matteo Masino, Dr. Gabriele Rispoli, Dr. Giulia Cantoni and Dr. Davide Capucci for their suggestions and help.

I would like to thank Prof. Leonard J. Barbour, Prof. Susan Bourne and Dr. Vincent Smith for allowing me to work in a fantastic team and to explore the city of Stellenbosch and Cape Town.

Thanks also to all the professors with whom I have collaborated and to all the students who have worked with me and who contributed to this PhD thesis.

Finally I would like to thank all the members of the Department of Chemistry of the University of Parma, including all the technicians, for their important support.